TESTS ON COLUMNS RESTRAINED BY BEAMS WITH SIMPLE CONNECTIONS

by

David J. Bergquist

This work has been carried out as a part of an investigation sponsored by the American Iron and Steel Institute, Project No. 189

Department of Civil Engineering
The University of Texas at Austin
Austin, Texas 78712

January 1977

Report No. 1

A C K N O W L E D G M E N T S

The research project whose results are reported herein was sponsored by the American Iron and Steel Institute. The guidance of the project advisory committee (R. Bjorhovde, W. Hansell, W. LeMessurier, L. Lu, J. Springfield) is greatly appreciated. The testing program was conducted at the Civil Engineering Structures Research Laboratory, Balcones Research Center, The University of Texas at Austin.

A B S T R A C T

Five tests were performed on a steel frame consisting of a column and four beams connected with simple connections. The purpose of these tests was to determine the effect of these simple connections on the buckling load of the column. The main variable was the connection type. In four of the tests the column was subjected to axial load only; in the fifth test a combination of axial load and lateral load was applied to the column. For all tests, buckling was about the weak axis. In addition, three tests were performed on beams to determine the moment-rotation characteristics of the connections.

In general, test results indicated that during column buckling only one beam provides restraint against rotation at a joint. Column web distortion in the vicinity of the connection significantly affected the buckling load. From the beam-column test it was found that the AISC interaction equations adequately predict the strength of the structure but that gross sway deflections occur at ultimate load.

A recommended design procedure is presented for the evaluation of the buckling load of columns restrained by beams with simple connections.

C O N T E N T S

L I S T O F T A B L E S

LIST OF FIGURES

CHAPTER 1

INTRODUCTION

1.1 Background

In continuous steel frames, columns may be subjected to axial load alone or a combination of axial load and moment. Regardless of the loading condition, the design equations for columns in the AISC Specification require the determination of the buckling load of the column. The buckling load is generally expressed in the form of the Euler buckling formula for a pinned-end column with an effective length of kL_c in place of the actual column length. The factor k is referred to as the effective length factor. The buckling load of a restrained column can then be expressed as

$$P_{cr} = \frac{\pi^2 EI_c}{(kL_c)^2} \tag{1.1}$$

where E is the modulus of elasticity, I_c is the moment of inertia of the column in the plane of buckling, and L_c is the unbraced length of the column.

Most engineers use the Jackson-Moreland alignment charts to obtain a reasonable value for the effective length factor[3*] in lieu of a difficult and often time-consuming exact solution. These alignment charts give the values of k factors as a function of the relative column-to-beam stiffness, G, for each end of the column. G is defined as

---

*Superscript numbers refer to the list of references.

$$G = \frac{\text{Column Stiffness}}{\text{Beam Stiffness}} = \frac{\Sigma(EI/L)\ \text{Columns}}{\Sigma(EI/L)\ \text{Beams}} \qquad (1.2)$$

where Σ indicates a summation of all members in the plane of buckling which frame into the joint under consideration. The beam-to-column connections at the joint are considered to be rigid.

In the AISC Specification, Type 2 construction is defined as construction where the beam-to-column connections offer no restraint to the beam against rotation for gravity loads. Such connections are permitted in unbraced frames if they provide adequate capacity to resist lateral loads.[1] These connections, designated as Type 2, do have some inherent rigidity. Consideration of this rigidity in the determination of k and P_{cr} would yield a higher buckling load than the one found using no restraint.

DeFalco and Marino[4] have developed a procedure for the determination of k accounting for the partial rigidity of Type 2 connections. This procedure involves the reduction of the beam stiffness to account for the connections used to evaluate G. The relative stiffness of a beam with Type 2 connections, R, is determined as

$$R = \frac{3}{4(L'/L) - (L/L')} \times \frac{I}{L} \qquad (1.3)$$

where $L' = L + 3EIZ$, L is the span of the beam, E is the modulus of elasticity, I is the moment of inertia of the beam, and Z is a measure of the moment-rotation characteristic of the connection. Equation (1.3) is then substituted into Eq. (1.2) in place of (I/L) beams. The flexibility factor, Z, is determined from the moment-rotation diagrams for the connections, as indicated in Fig. 1.1. It is the inverse of the initial elastic stiffness of the connection. A large Z value means that the connection is very flexible. Values of Z used by DeFalco were obtained using equations developed by Lothers.[6] In the determination of k, all beams framing

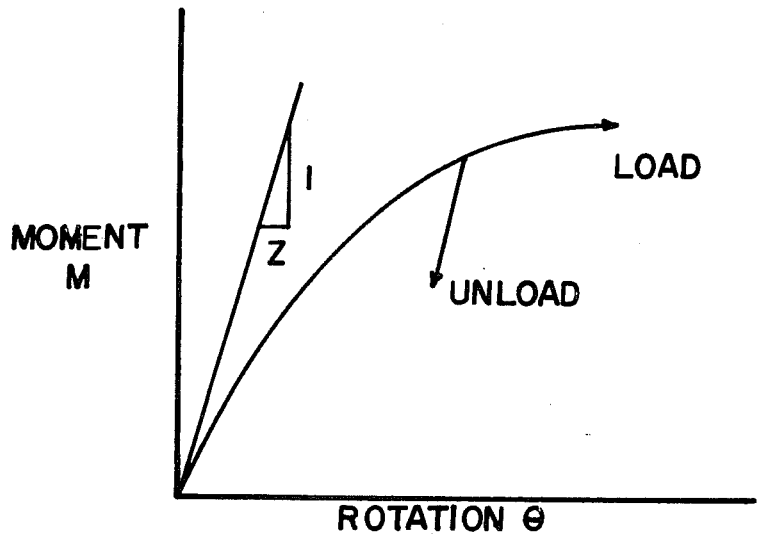

Fig. 1.1 Moment-rotation characteristics of Type 2 Connection

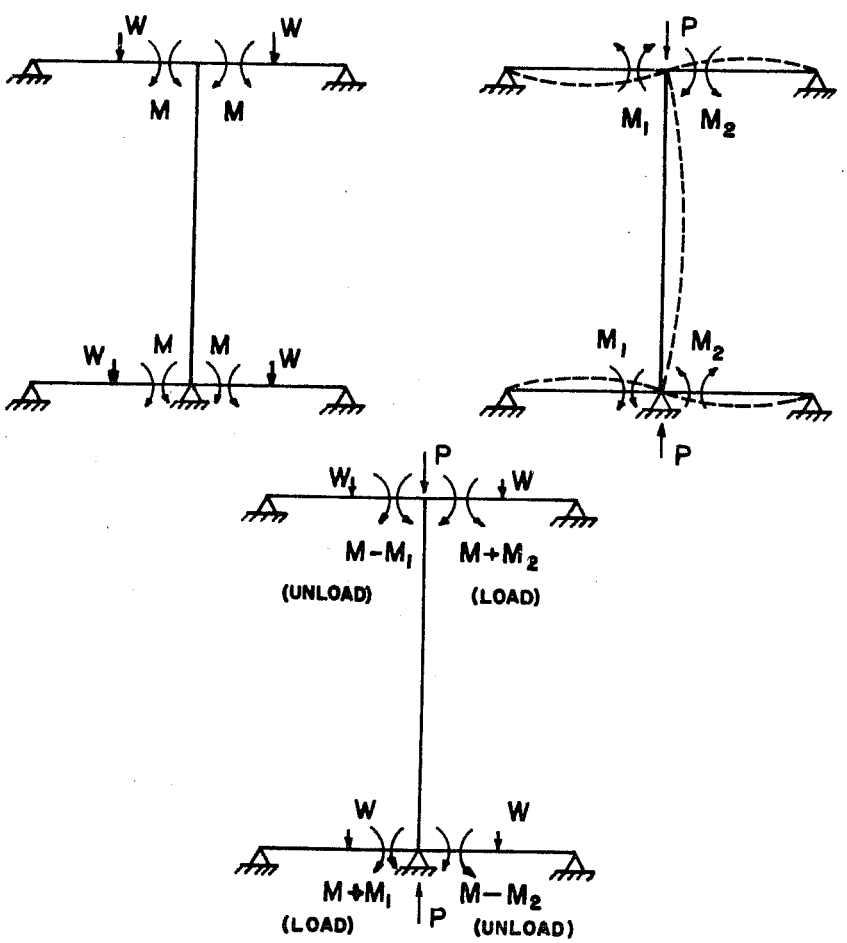

Fig. 1.2 Result of joint rotation during buckling on the magnitude of beam moments

into the joint in the plane of buckling are considered to offer restraint.

Complications arise if the effect of joint rotation during buckling on the magnitude of beam moments is considered. Figure 1.2 shows that during joint rotation the beam moment on one side of the joint increases while the beam moment on the other decreases. From Fig. 1.1 it is seen that when the connection unloads it does so along a line of a certain stiffness. The connection that continues to load, though, does so along a line of about zero stiffness. This would indicate that only one beam is restraining at a joint during joint rotation, whether the rotation is due to buckling or bending due to a lateral load. From this discussion it is also apparent that the unloading characteristics of the connection must be known. This characteristic will be expressed as the unloading flexibility factor, Z-unload. It is apparent that this partial rigidity should also be taken into account for beam-columns with Type 2 connections.

1.2 Purpose and Scope

As can be seen from the above discussion, there is much confusing theoretical information on the topic of columns restrained by beams with Type 2 connections. Values of the elastic flexibility factor, Z-elastic, obtained using Lothers' technique agree favorably with test results,[6] but no experimental evidence is available for columns restrained by beams with these "simple" connections. A test program was undertaken to study this topic.

Five tests were performed on W10X29 columns. One of these tests was a pinned-end column test to determine the Euler buckling load. In the remaining four tests, the columns were restrained by two beams framing into the top and bottom, utilizing Type 2 connections. Three of the tests were buckling tests with axial load alone. These three tests utilized three different Type 2

connections. The fourth test was a laterally loaded beam-column in which the column was subjected to a combination of axial and lateral load. For each of the connections used, separate connection tests were performed to determine their moment-rotation characteristics.

A theoretical study was also undertaken to account for the partially rigid connections in an "exact" buckling analysis. The experimental results and theoretical study are used to develop design recommendations for finding the buckling load of columns restrained by beams with Type 2 connections.

CHAPTER 2

TEST PROGRAM

Four tests were performed on single columns restrained by beams to determine the effect of three different beam-to-column shear connections on column behavior. Three of the tests assessed the buckling strength of the axially loaded restrained column with the connection type being the principal variable. In the fourth test, the column was subjected to combined axial load and moment. In addition, tests were performed to determine the moment-rotation characteristics of the connections. Framing angles connected the beam web to the column web for all tests. The three connection types were: (a) angles bolted to beam and column web; (b) angles bolted to beam web, welded to column web; and (c) angles welded to beam web, bolted to column web.

Figure 2.1 shows the loading arrangement for the buckling tests. Dashed lines indicate the specimen's shape in its buckled configuration. The beam-column specimen was tested with an additional load, shown dashed to simulate lateral load. As seen in Fig. 2.1(b), the specimen could be thought of as representing a portion of a fixed base unbraced frame with the column's centerline simulating a fixed base. However, for the purposes of analysis, each specimen was treated as a braced frame consisting of a column braced at both ends by beams using flexible connections designed for shear only (designated as Type 2 construction by the AISC Specification). The results of all tests could then be used to determine the effects of "simple" connections on the column's stability and strength.

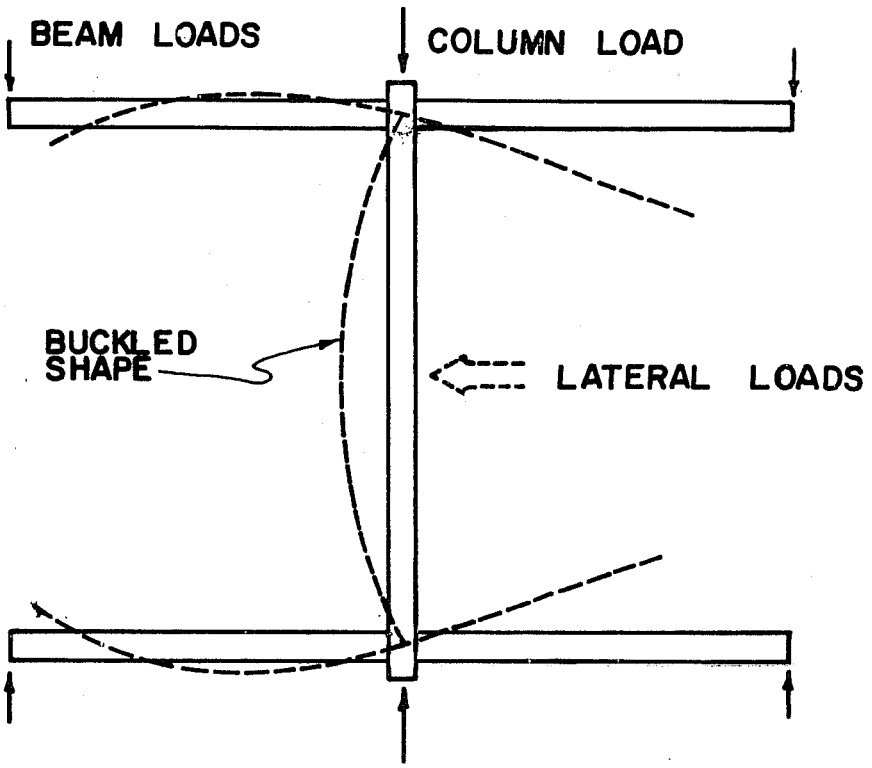

(a) Typical specimen--plan view

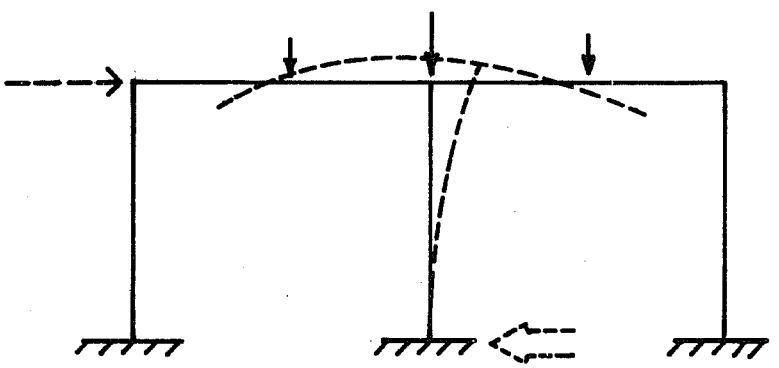

(b) Portion of actual frame simulated by test specimen

Fig. 2.1 Test program--loading scheme

2.1 Design of Specimens

The test equipment available limited the applied column load to a maximum of 220 kips. A theoretical study using a W10x29 column section which was available was undertaken to check its suitability. The procedure presented by DeFalco and Marino and discussed in Chapter 1 was used in the theoretical study. Pilot tests were performed using connection angles with two different thicknesses (1/4 in. and 3/8 in.) to obtain values for Z, the flexibility factor, to be used in the theoretical analysis. Based on this theoretical study and the pilot tests, W10x21 beam sections and 4 in. x 3-1/2 in. x 1/4 in. connection angles with specified minimum yield strengths of 36 ksi, and a W10x29 column section with a specified minimum yield strength of 50 ksi were chosen. Figure 2.2 shows the lengths and orientation of the members for each specimen. For each specimen, flexible web angle connections were used for the beam-to-column joints. Where the angles were bolted, 7/8 in. A325 bolts were tightened with an impact wrench, using the turn of the nut method. Where the angles were welded, 3/16 in. fillet welds using E70 electrodes were used. Three connection types were used in order to determine the effect of the connections on the moment-rotation characteristics of the connections and the buckling load of the column. Figure 2.3 illustrates the three connection details used.

The column was designed on the basis of weak axis buckling, as this would eliminate the need for bracing out of the plane of the test frame. The columns were designed for elastic buckling in Tests I, II, and III. Any increase in the buckling load above the Euler buckling load could be attributed to restraint from the beams and not residual stresses or inelastic column behavior. Keeping the column elastic reduced the number of members required, since the same column could be used for more than one test. In addition, auxiliary column information, such as yield strain and

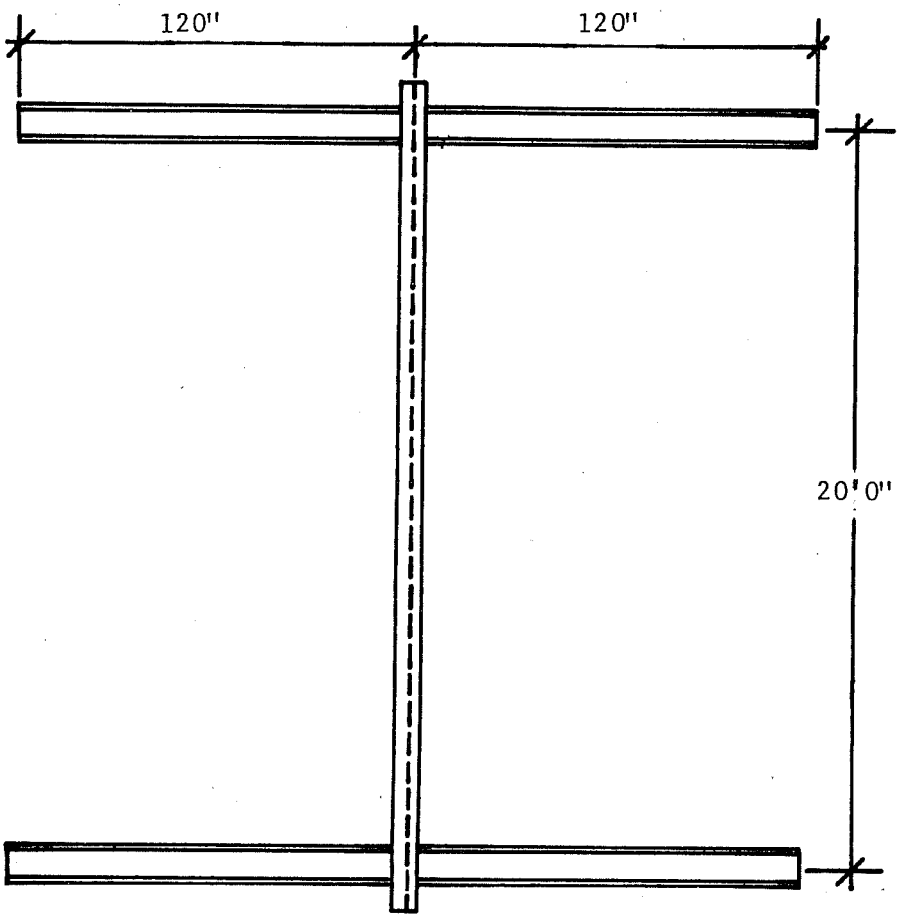

Fig. 2.2 Final design of specimens, plan view

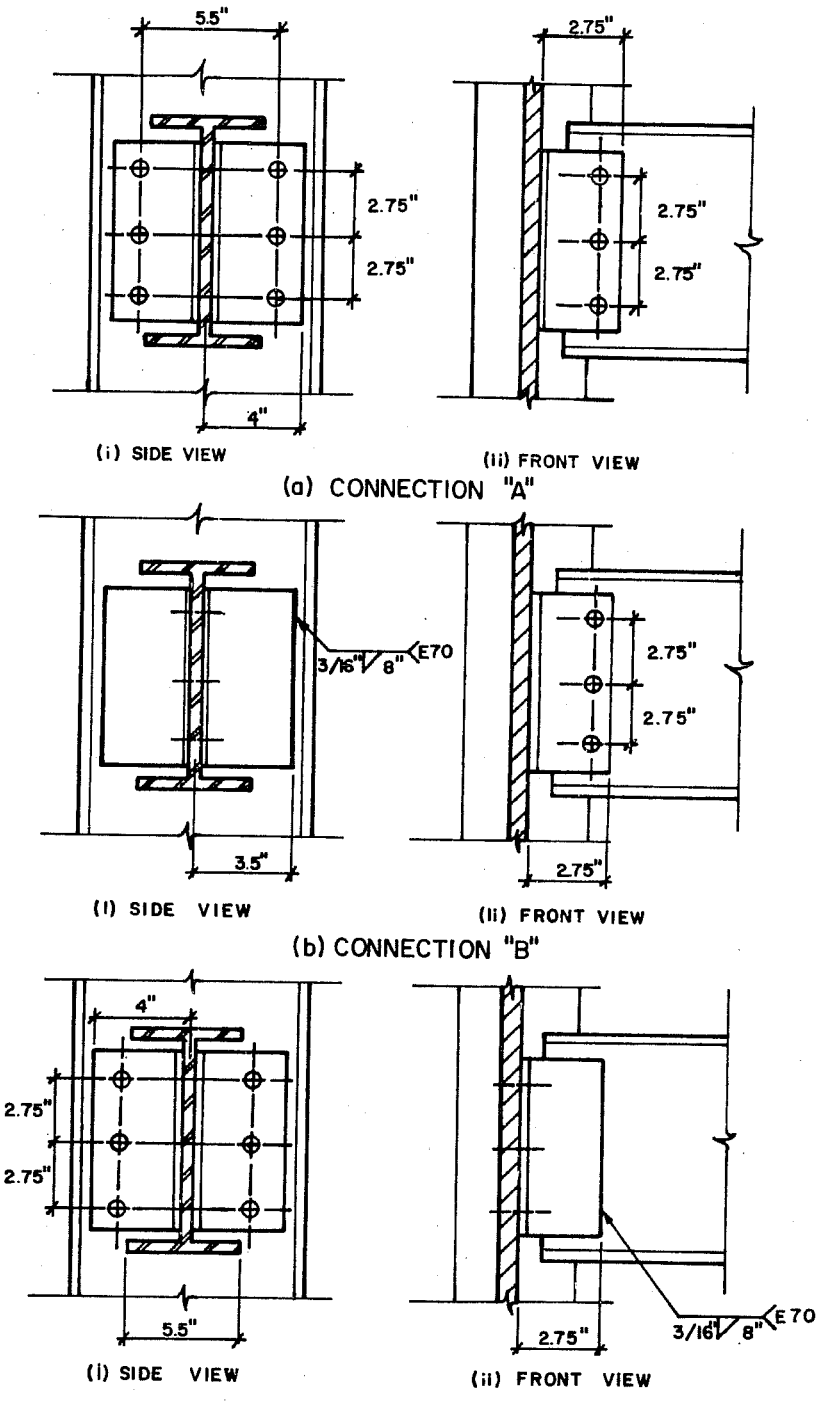

Fig. 2.3 "Simple" connection details

magnitude and distribution of residual stresses would not be needed, since these factors do not affect elastic column buckling. In Test IV, the column was loaded beyond elastic behavior, but this was done through the application of a lateral load, not through a classical buckling phenomenom.

Table 2.1 summarizes the final designs of the specimens for Tests I through IV, and Connections A, B, and C.

2.2 Test Setup

For all of the tests the plane of the test specimen frame was horizontal. Axial load on the column was applied by a 100-ton hydraulic ram (10 in. stroke) operated by a hand pump. The test setup was designed to accommodate a total column length of 21 ft., 6 in. End plates were welded to the column to which machine-grooved plates could be bolted. The column loads were applied through the use of knife-edges (at each column end) which were mated to the groove plates. Use of the knife-edges prevented development of a moment at the column ends as they rotated during buckling. However, the 0.25 in. deep groove and knife-edge combination and its lateral support was capable of resisting any shears that developed during the application of load, thus preventing the column from translating laterally as a whole. The axial load was transmitted from the column to reaction beams (at each end) which were supported by two reaction brackets prestressed to the test slab. Typical details of one end of the loading system are shown in Fig. 2.4. In general, the details are identical for the other end of the column except that a 200-ton load cell for monitoring axial load was used in place of the 100-ton ram. The columns were vertically supported initially by screw jacks at each end. Adjustment of the screw jacks permitted vertical alignment of the column so that no eccentricities of load would be present in the strong direction.

TABLE 2.1 FINAL DESIGN OF SPECIMENS

Member	Test Number	Section	Minimum Specified Yield Strength	Length	Buckling or Bending Axis
Column C1	I & IV	W10X29	50 ksi	20' - 0"	Weak
Column C2	II & III	W10x29	50 ksi	20' - 0"	Weak
Beams	All Tests	W10X21	36 ksi	10' - 0"	Strong

Connection Type	Test Number	Angle Type	Length	Beam Web Connector	Column Web Connector
A	I & IV	4"X3-1/2"X1/4"	8"	7/8"Ø A325 bolts	7/8"Ø A325 bolts
B	II	4"X3-1/2"X1/4"	8"	7/8"Ø A325 bolts	3/16" E-70 fillet weld
C	III	4"X3-1/2"X1/4"	8"	3/16" E-70 fillet weld	7/8"Ø A325 bolts

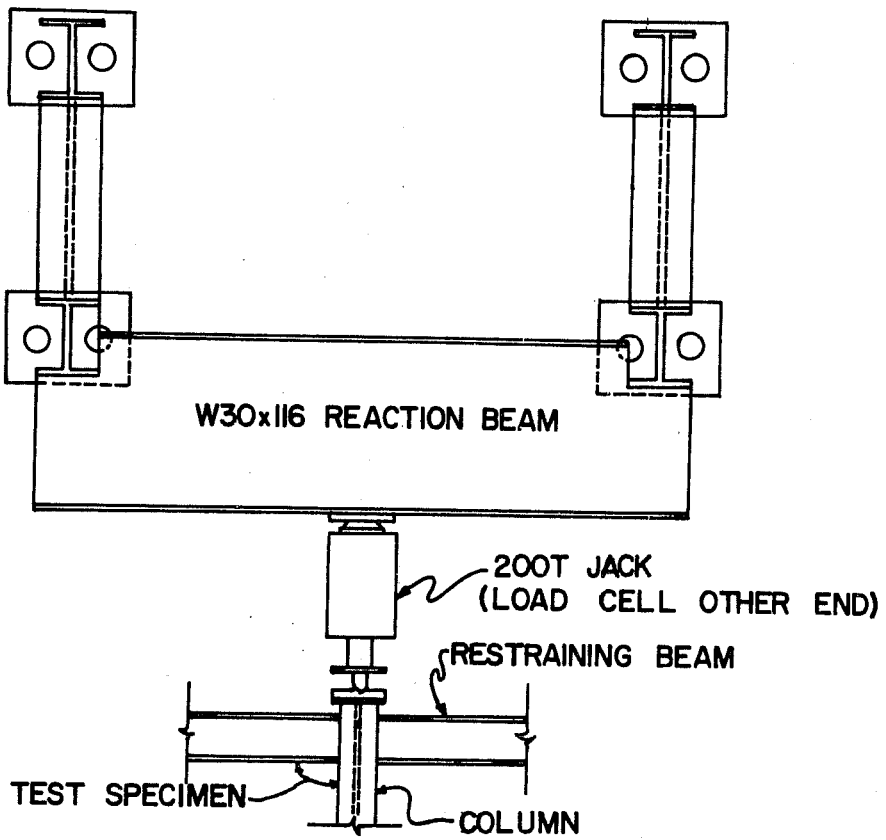

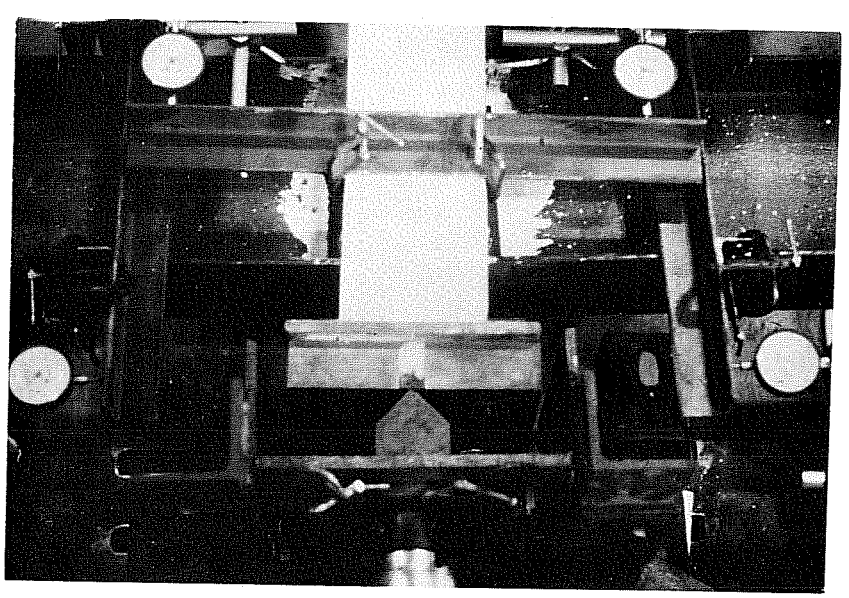

Fig. 2.4 Details of column loading system

Figure 2.5 illustrates the arrangement of the beam loading system. Beam loads were applied through a self-contained system of a 12-kip hydraulic tension ram (24 in. stroke), a 1 in. threaded rod, and a 10-kip tension load cell connected in series and attached to the beam ends through a clevis bracket. The two tension rams shown in the figure were operated by the same hand pump through the use of intermediate manifolds. Shut-off valves were attached at the rams, which permitted independent operation of either ram as well as the capacity to hold the rams in a desired position. With all valves open the load in the rams was essentially equal. By closing one set, it was possible to load one of the rams independently. Finally, by closing both sets of valves the positions of the ends of the beams could be held, since hydraulic fluid could not flow either into or away from the rams. Vertical support for the beams was provided near the ends by angles parallel to the beam webs. In order to minimize friction at these locations, rollers were provided between the beam webs and the angles. These rollers consisted of needle bearings within aluminum cylinders slipped onto the shaft of commercial swivel casters. Tests performed on the rollers indicated that a horizontal force of 8 lbs. was required to overcome the static friction induced by a vertical force of 300 lbs.[8]

The lateral loading for the beam-column test required additional apparatus. The lateral loading unit consisted of a Universal load cell attached to the column web (at the column centerline) and to an auxiliary frame prestressed to the test slab with two threaded rods. The load was applied through deformation control by tightening or loosening the nuts. This apparatus is shown in Fig. 2.6. Also, two additional supports were attached to the ends of the beams, because there was a possibility that the force in the tie rod system could become compressive. Since the tie rod could support very little compression, the beam end support could be lost without additional supports. This additional support was achieved through

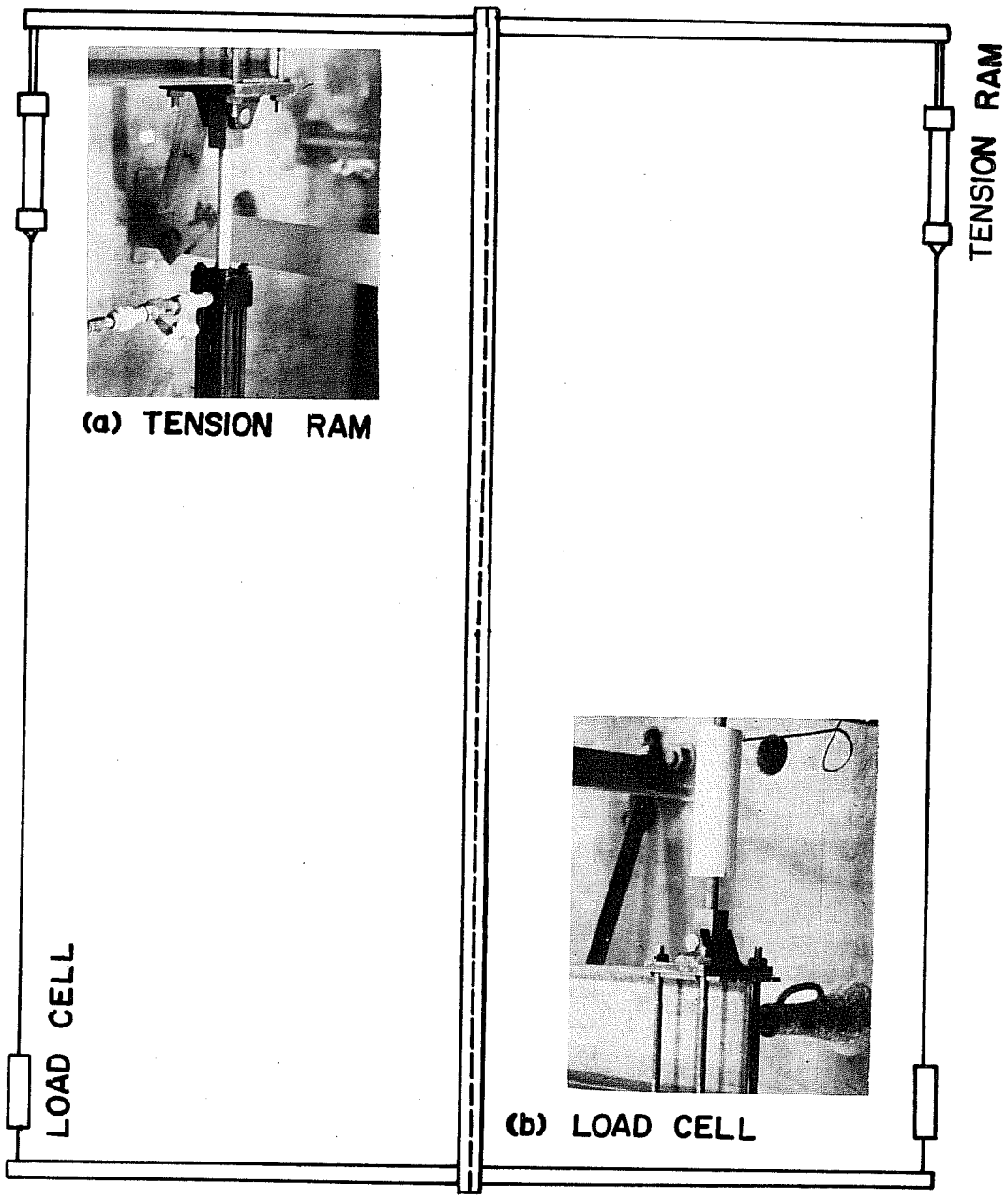

Fig. 2.5 Self-contained beam loading system

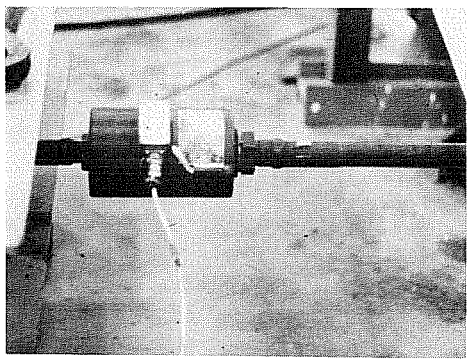

(a) Universal load cell

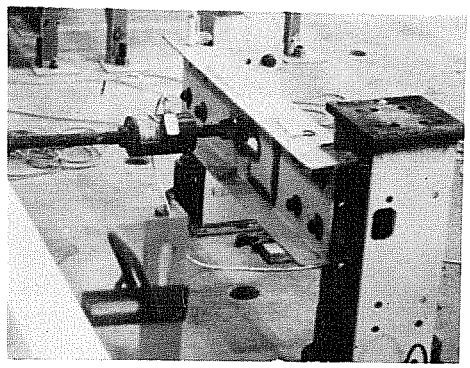

(b) Lateral load bracket

Fig. 2.6 Lateral load system

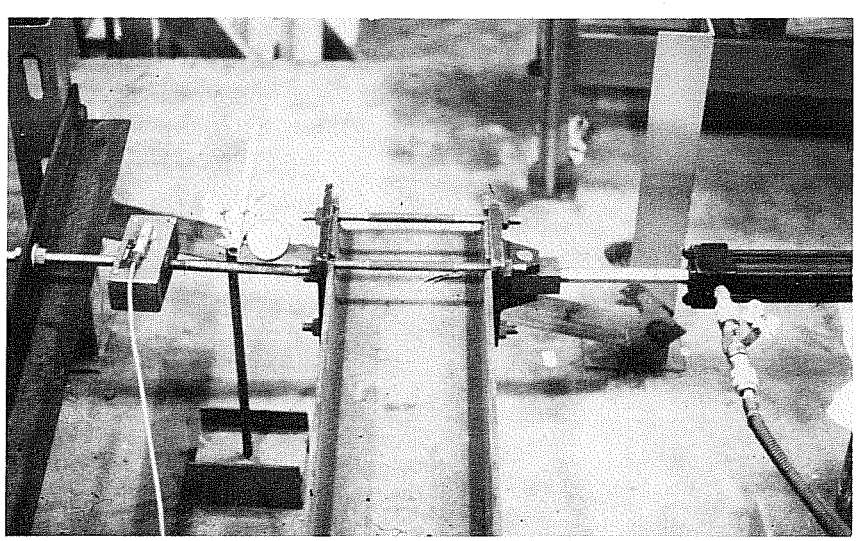

Fig. 2.7 Additional load cell

the use of additional load cells and threaded rods attached to auxiliary frames. Figure 2.7 shows a typical detail of these load cells used to record load in the secondary beam support system.

2.3 Instrumentation

Column axial loads were measured by a load cell calibrated to 240 kips. Beam loads were measured by load cells which were calibrated to 12 kips. Figure 2.5 shows the relative positions of the two tension load cells used in measurement of the beam loads. The additional load cells used to measure the reversed loads in the unloading beams were calibrated to 20 kips and are shown in Fig. 2.7 Column loads were considered accurate to within 0.3 kips and beam loads were accurate within 0.015 kips. As a check on loads measured by the load cells, loads were determined from pressure transducers and pressure gages connected to the hydraulic system. No differences of over 3 percent between load readings were observed; therefore, only loads from the load cell readings were reported as they are considered to be the most accurate. Lateral loads were measured by a Universal load cell calibrated to 30 kips and were considered accurate to within 0.02 kips.

Dial gages reading to 0.001 in. were used to measure column translations, beam end deflections, and beam and column end rotations. Rotations were measured using two dial gages, one at each end of a 20-in. piece of angle rigidly attached to the ends of the beams and column. By dividing the difference between the two dial gage readings by 20 in., the rotation in radians was determined. The relative locations of the dial gages can be seen in Fig. 2.8.

The initial column centerline deflection and shape were determined by the use of a transit sighting on a scale graduated in 1/32 in. These transit readings were considered accurate to 1/32 in. Prior to each test, the line of sight of the transit was made

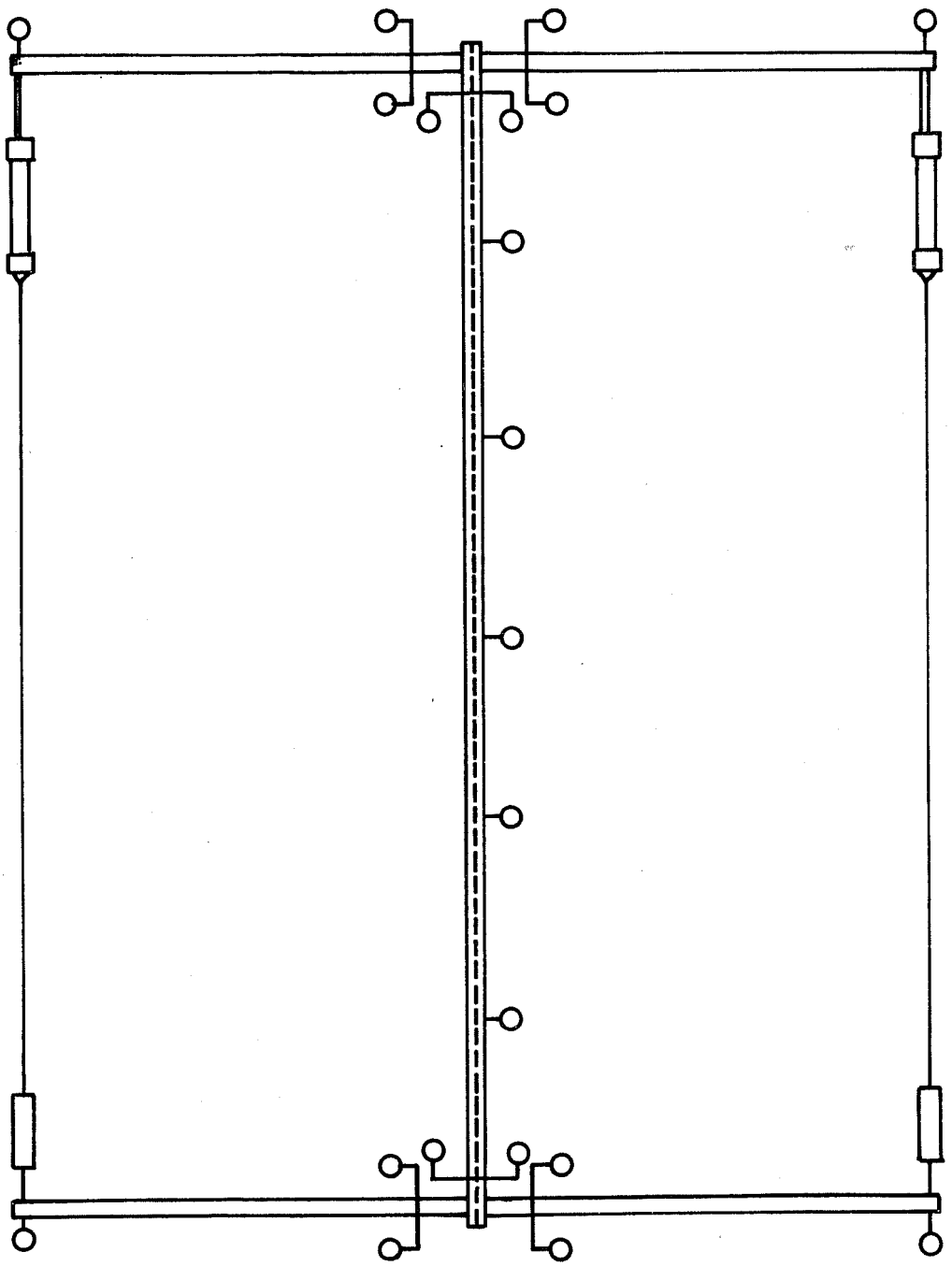

Fig. 2.8 Dial gage locations

parallel to an imaginary line between the knife edges at each column end. Readings on the scale at the knife edges and at the dial gage locations along the column sighted by the transit before the application of any loads enabled the determination of the initial eccentricity of the column, Δ_o, and the column's initial shape.

2.4 Cross Section and Material Properties

As shown in Table 2.1, W10X29 columns with a specified minimum yield strength of 50 ksi were used for all specimens. All columns had been cold-straightened by a continuous rotarizing process as part of the normal mill-rolling process.

Since only the column used in Test IV (C1) was to be loaded to a stress level higher than the yield stress, it was necessary to determine its material properties from tension coupon tests. The column was used previously in a test program carried out at The University of Texas at Austin and was not yielded. The properties of the specimen were obtained from the report of this test program[5] and are presented in Table 2.2, along with the properties of the other column section and the beams.

Cross section dimensions for both column members (C1 and C2) were measured at the two ends and at the column centerline. Thicknesses were measured using a micrometer and were read to 0.001 in. Widths and depths were measured using a set of Yankee Spring dividers and scale graduated to 0.01 in. In general, average values from the three measurement locations were calculated for the various dimensions. Based on these average values, cross-sectional properties were calculated neglecting the fillets. A summary of these measured values and those given by AISC can be found in Table 2.2.

One column test without beams was performed on column C1 in order to determine its Euler buckling load. Results of the test are shown in Fig. 2.9. The behavior is represented by a plot of

TABLE 2.2 CROSS-SECTIONAL PROPERTIES

Member	Area ($in.^2$)	d (in.)	b_f (in.)	t_f (in.)	t_w (in.)	I* ($in.^4$)	M_p (kip-in.)
Column							
C_1(W10x29)**	8.79	10.17	5.825	0.506	0.316	16.7	466
C_2(W10x29)	8.51	10.17	5.844	0.502	0.289	16.7	---
AISC	8.54	10.22	5.799	0.500	0.289	16.3	431+
Beams							
W10x21 (AISC)	6.20	9.90	5.75	0.340	0.240	10.7	---

*Moment of inertia in plane of buckling for column (weak direction); in plane of bending for beams (strong direction)

**From Ref. 5.

+Based on nominal yield strength

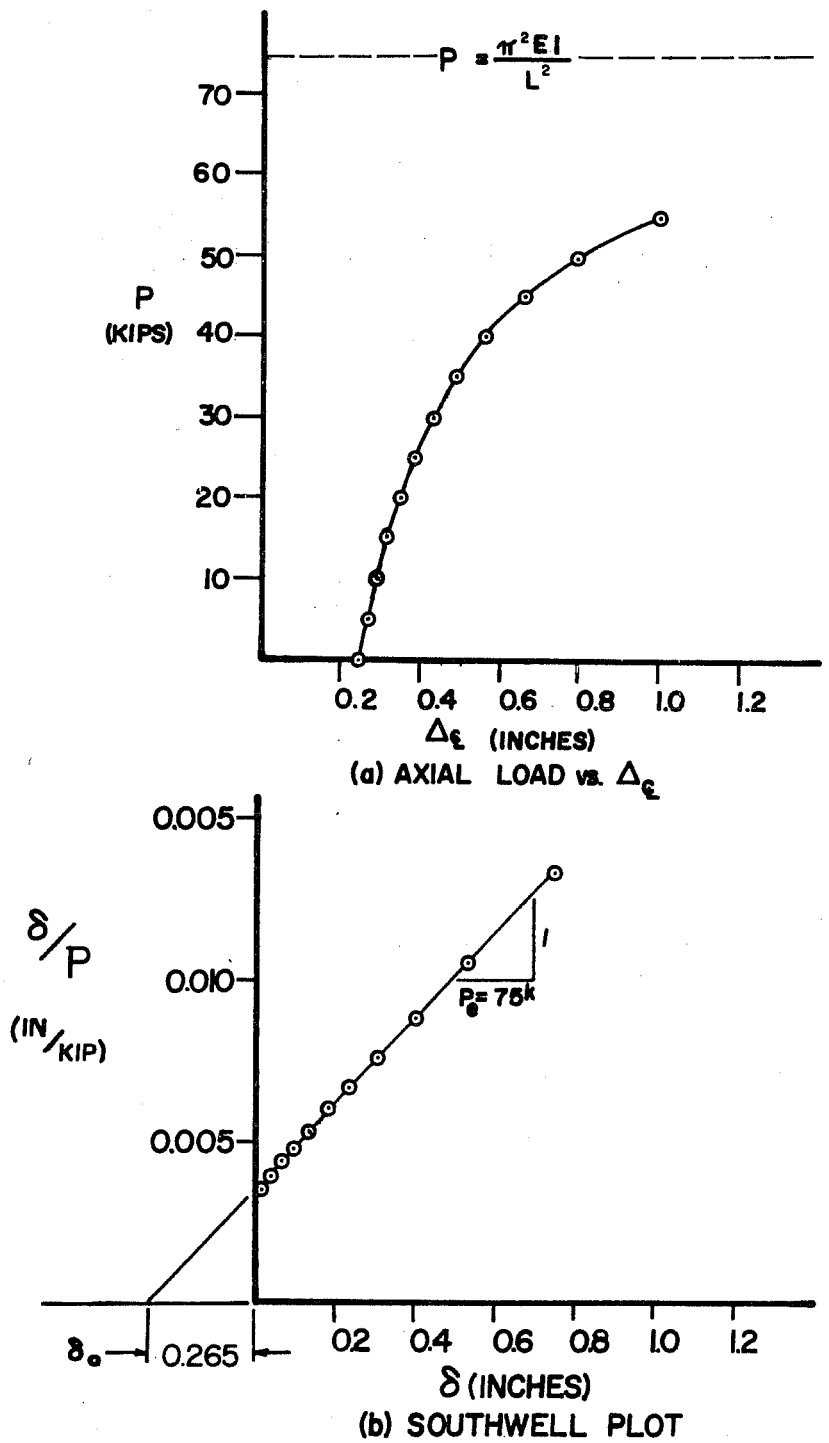

Fig. 2.9 Results of Euler test

axial load versus centerline deflection, and the Euler load was determined from a Southwell plot. Using this method, δ/P is plotted against δ, where δ is the column centerline deflection due to the application of axial load P. The elastic buckling load can then be determined as the inverse of the slope of the line which passes through the points plotted at each load stage.[10] The intercept of this line with the x-axis is related to the initial eccentricity and the end load eccentricity of the column. Use of the Southwell plot permitted the determination of the elastic buckling load without actually reaching this load level in the test. Using the Euler load from the test and the formula for determining the Euler load ($P_E = \pi^2 EI/L^2$), it was possible to determine a test value for the EI of the member equal to 5.2×10^5 kip-in.^{2}. Also, the Euler load (when adjusted for different lengths) could be used as a basis for determining the effect of the restraining members on the buckling load of the column. For the column 21 ft., 10 in. long, the Euler load from the test was 75 kips; for the 20 ft. column, the Euler buckling load would be $P_E = 75k \times (262 \text{ in.}^2/240 \text{ in.}^2) = 89$ kips.

2.5 Moment Rotation Characteristics of the Connections

Three tests were performed on beams with the three types of connections discussed earlier in order to obtain the moment-rotation characteristics of the connections. A description and drawing of the test setup is presented in Appendix B. Results of the tests are shown in Fig. 2.10. The behavior is represented by a plot of beam moment, nondimensionalized with respect to the M_p of the beam, versus connection rotation. Connection rotation is defined as the relative rotation of the column end of the beam with respect to the column. Beam moment was determined as the product of the ram load times the distance from the column face to the centerline of the loading ram. The inverse of the slope of the initial loading portion of the curve is defined as the elastic flexibility factor, Z_E.

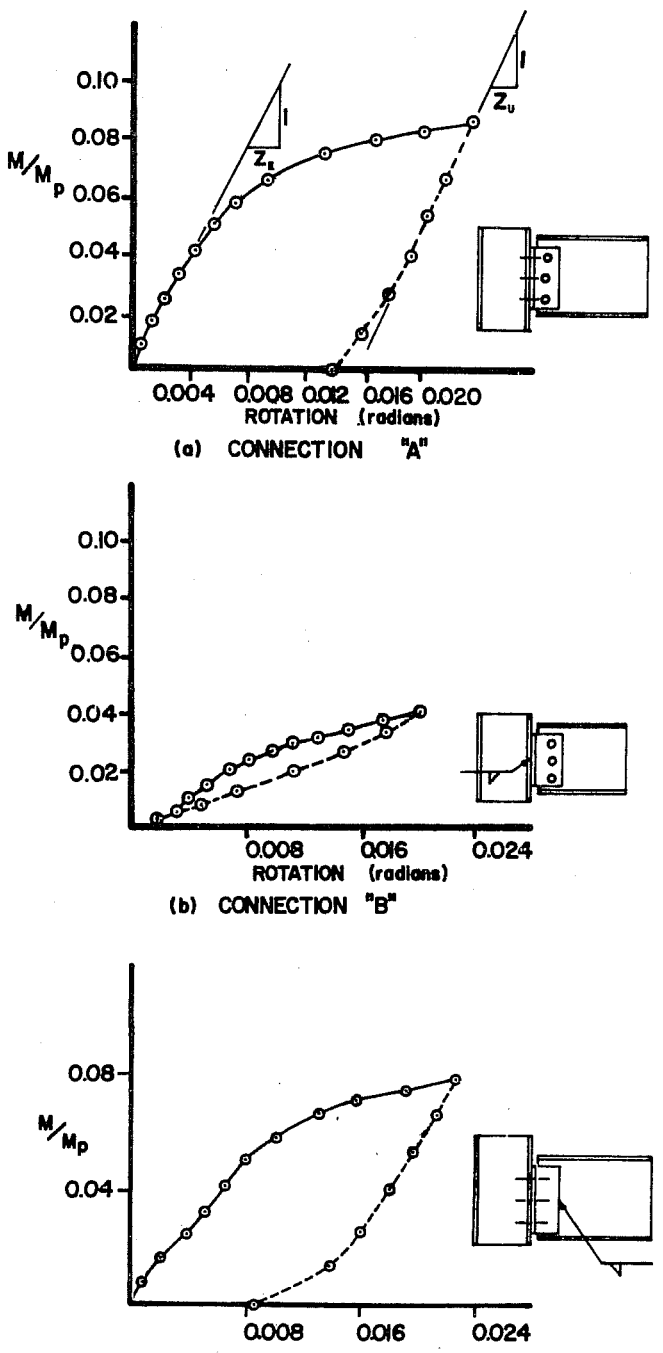

Fig. 2.10 Moment-rotation characteristics

The inverse of the slope of the unloading curve is defined as the unloading flexibility factor, Z_U. The flexibility factors for each test are presented in Table 2.3

TABLE 2.3 FLEXIBILITY FACTORS OF CONNECTION TYPES A, B, AND C FROM MOMENT-ROTATION TESTS

Connection Type	Test Number	Elastic Z_E (rad/k-in.)	Unloading Z_U (rad/k-in.)
A	M-θ(1)	0.94×10^{-4}	1.1×10^{-4}
B	M-θ(2)	5.7×10^{-4}	5.2×10^{-4}
C	M-θ(3)	1.4×10^{-4}	1.4×10^{-4}

2.6 Test Procedure

Each specimen was aligned geometrically through the use of a transit. Lines of sight were established through which the 100-ton ram, the column ends, and the axial load cell were aligned longitudinally. Vertical alignment also utilized the transit through a leveling procedure. These procedures were also used to determine the initial camber and sweep of the column so that eccentricities of axial load could be determined.

All of the buckling tests began with the introduction of a small axial load (about 5 kips) into the column to allow the specimen and fixtures to settle into place and to permit removal of the screw jacks supporting the ends of the column. Next, beam loads were applied to the beams until a rotation of about 0.017 radians. This rotation corresponds to the rotation that would occur at the end of a simply supported beam with a typical span of 20 ft. and typical load of 1 kip per ft. of span. Beam loads were applied in several increments

until the desired rotation was reached. At each stage, beam loads were measured and recorded along with beam end deflections, joint rotations, and column translations (at five points along its length, including centerline deflection). Initial stages of beam loads were applied equally to all beams by leaving all of the shut-off valves at the rams open. For the three stability tests (I, II, and III), this procedure was carried out through the final stages until the desired rotation was reached. In Test IV, uneven friction caused the beams on one side to reach the desired rotation before the other beams. In this case, once the beams on one side reached the desired rotation their shut-off valves were closed and the other beams were loaded independently up to the final rotation. When the desired rotation was reached in all the beams, all shut-off valves were closed. In general, the beam moments did not differ by more than 2 percent after the final beam loading.

The next phase was to load the column axially until the buckling load could be determined. At each increment of column axial load the following data were recorded: column axial load, column translation, joint rotations (both column and beams), beam loads, and beam end deflections. For Tests I, II, and III, the column axial load was increased until a preliminary Southwell plot (discussed earlier), drawn from the raw data during the test, showed reasonable linearity. The column centerline deflection was to be held less than that deflection at which yielding would occur in the cross section, but the previous criterion always governed the procedure.

For the beam-column test, the beam loading was as discussed above. However, the column load was stopped when the axial load reached 41 percent of the buckling load determined from the stability test. This level of axial load was then held reasonably constant as lateral load was applied. During the application of lateral load, all of the above data were recorded as well as the lateral load at

each stage. The lateral load was increased in increments until an instability was encountered (increasing centerline deflection with no increase in load), then a few more load stages were applied to determine the unloading characteristics of the specimen.

CHAPTER 3

TEST RESULTS

In this chapter the results of the four restrained column tests will be presented. The following definitions are for terms which will be used in the presentation of results and discussion for each test:

P_{cr} = buckling load from Southwell plot

P_{max} = maximum applied axial load

M_o = beam moment at start of column loading

M_p = plastic moment capacity as listed in the AISC Manual

δ = deflection at column centerline due to applied beam loads and column loads

δ_o = initial column centerline eccentricity measured from a line between the geometric centers of the joints

$\Delta_{\text{℄}}$ = column centerline deflection measured from a line between the geometric center of each joint equal to $\delta_o + \delta$ at each load stage

H_{max} = maximum applied lateral load

3.1 General

Figure 3.1 illustrates the various deflections and loading stages. For each test, the beam behavior is represented by plots of nondimensionalized beam moment, M/M_p, versus beam rotation relative to the end of the column, θ. M was determined by multiplying the measured beam load by the distance from the column web to the centerline of the beam loading system. The values of the beam moments for each experiment are presented with respect to the M_p = 72.3 kip-ft. for the W10x21 specimen as it is listed in the AISC Manual.[1]

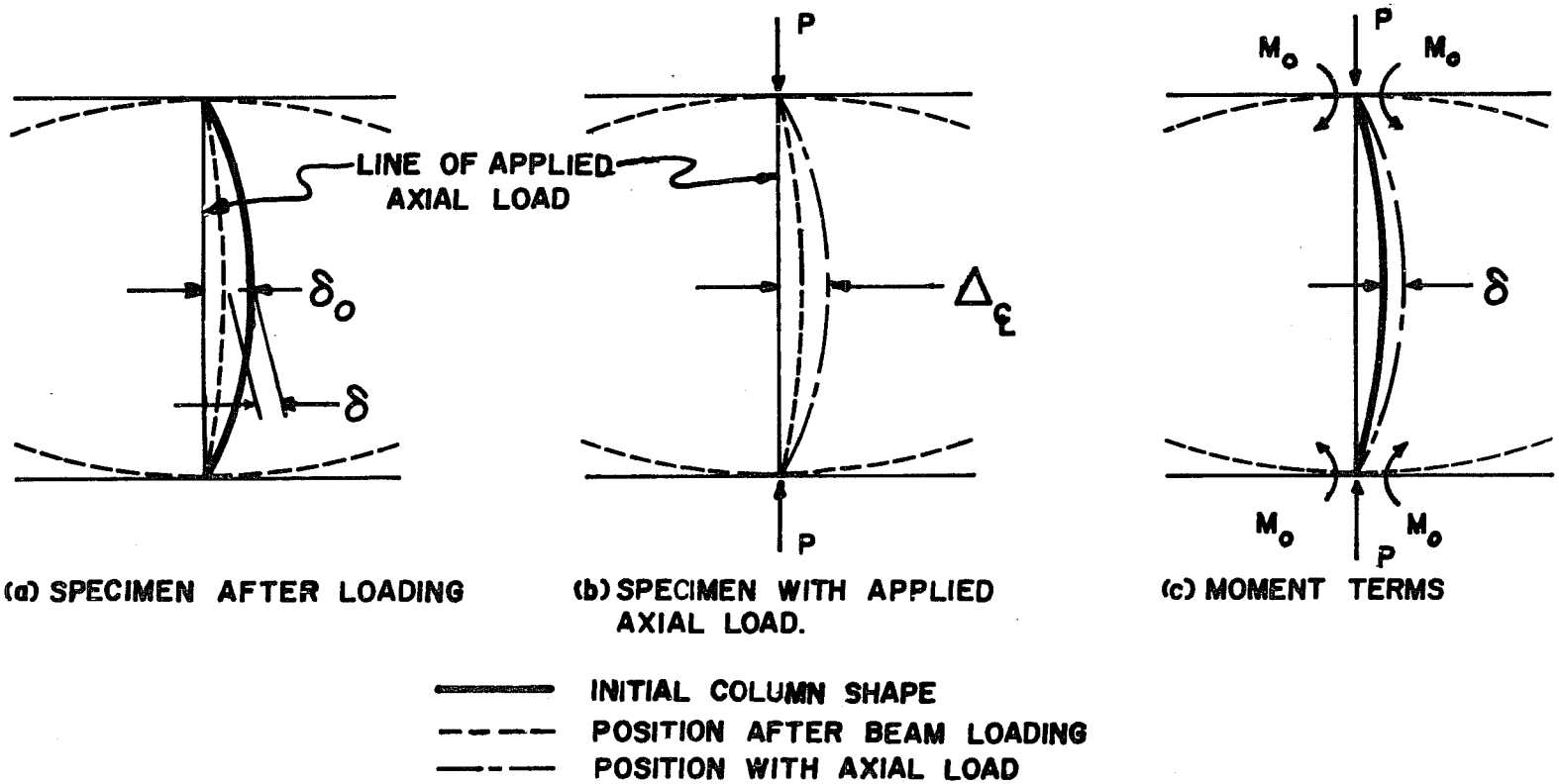

Fig. 3.1 Deflections at different stages of loading

Column behavior for each test is represented by plots of axial load, P, versus centerline deflection, $\Delta_{\mathfrak{C}}$. Due to the self-contained nature of the beam loading system, P at each load stage was determined as the sum of the beam loads plus the externally applied column load. P_{cr} for each test was determined from a Southwell plot (discussed in Chapter 1) with the data points for each load stage plotted as δ/P versus δ. P_{cr} was determined by a least-squares straight line fit to the last five data points. The early data points were generally not considered to be reliable, due to the effects of small restraints and seating of the test setup as well as experimental error, all of which are more pronounced at low levels of axial load and deflection. For this reason, only the last five data points, which appeared to be on a reasonably straight line, were used in evaluating P_{cr} for each test.

The column in Test IV was subjected to beam loads, column axial load, and lateral load. For this test an additional plot of lateral load versus $\Delta_{\mathfrak{C}}$ is used to represent the behavior of the specimen.

3.2 Results of Test I

The results of Test I are included in Table 3.1 and Figs. 3.2 through 3.4. In this test the connecting angles were bolted to both the beam and column webs, as shown in Fig. 2.3(a). The plots in Figs. 3.2 and 3.3 illustrate the behavior of the beams as they rotate under various levels of moment. The general behavior of the beams up to M_o is the same for all the beams; that is, when the first increments of moment are introduced, the beam responds elastically and the plot is linear. The scope of this linear portion of the curve is referred to as the elastic stiffness. Upon further application of moment, the stiffness deteriorates until the curve is generally flat at the desired level of rotation corresponding to M_o. At this point the stiffness would be considered to

TABLE 3.1 TEST RESULTS

Test	M_p-beam (kip-ft.)	M_o/M_p west	M_o/M_p east	P_{cr} (kips)	P_{max} (kips)	δ_o (in.)	H_{max} (kips)
I	72.3	0.078	0.074	123	105.2	0.1875	---
II	72.3	0.0253	0.0252	103	78.7	0.1875	---
III	72.3	0.0676	0.0685	118	91.8	0.1875	---
IV	72.3	0.0864	0.0864	---	51.3	0.1875	4.49

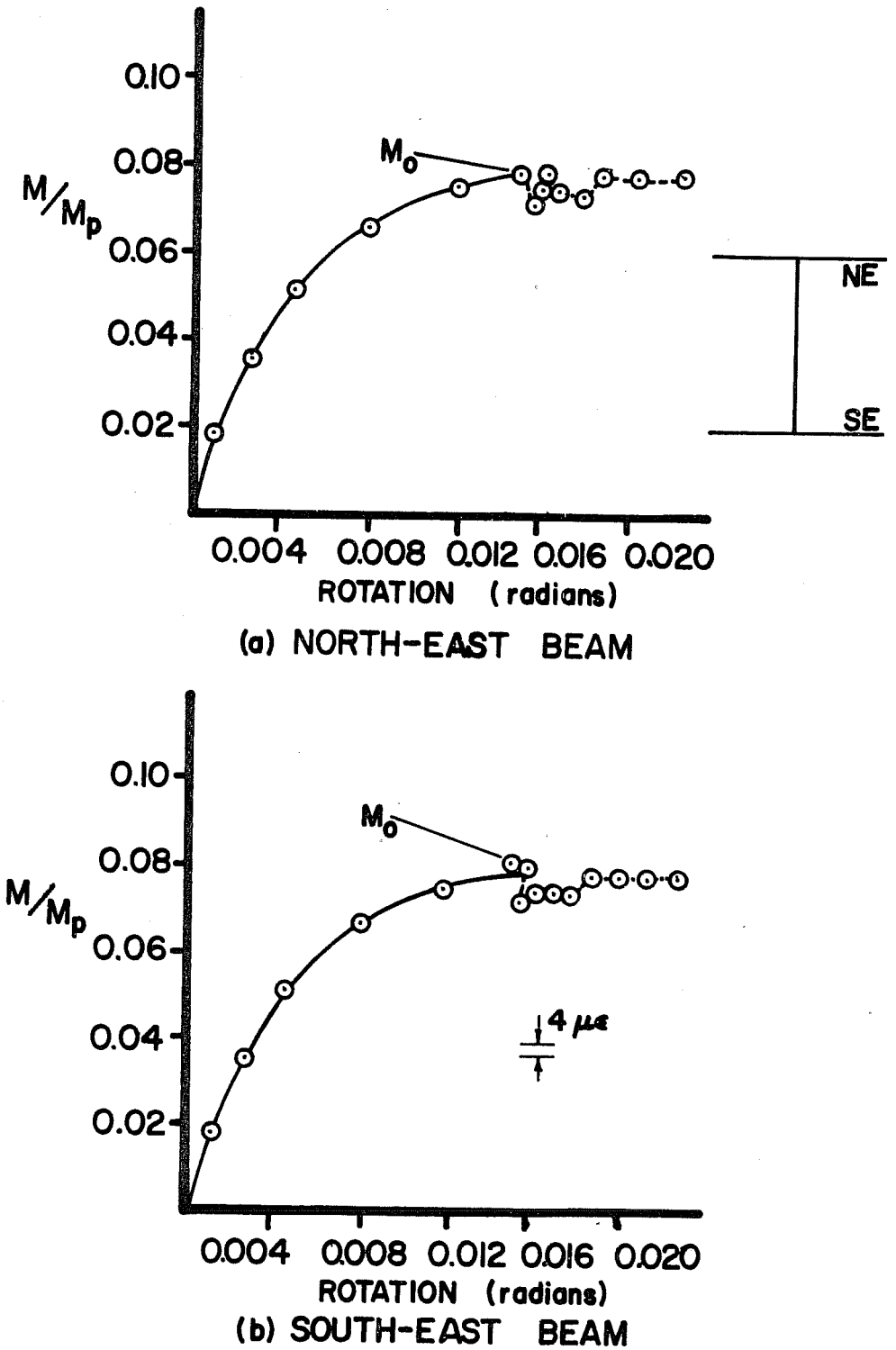

Fig. 3.2 Beam behavior--Test I

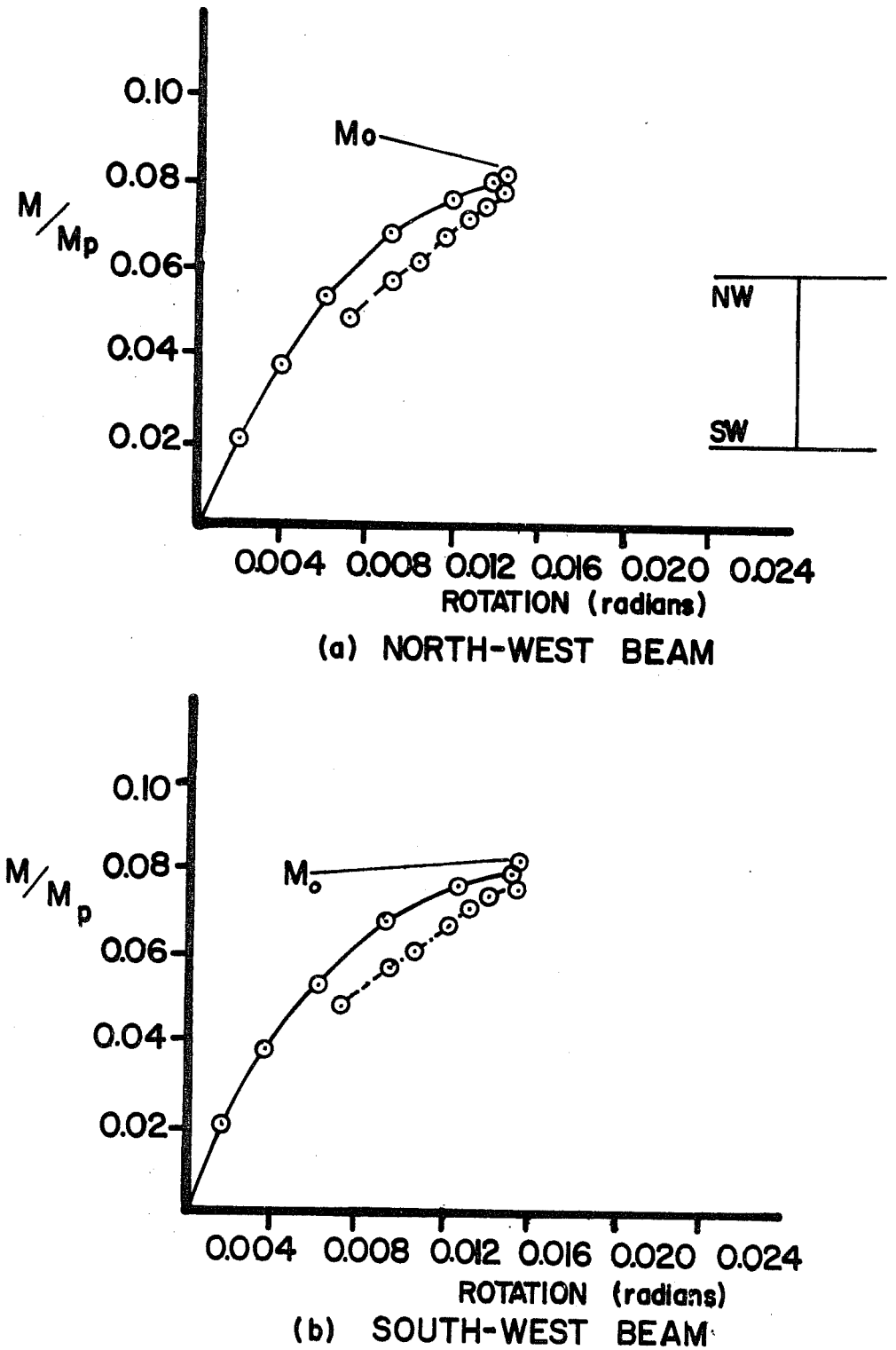

Fig. 3.3 Beam behavior--Test I

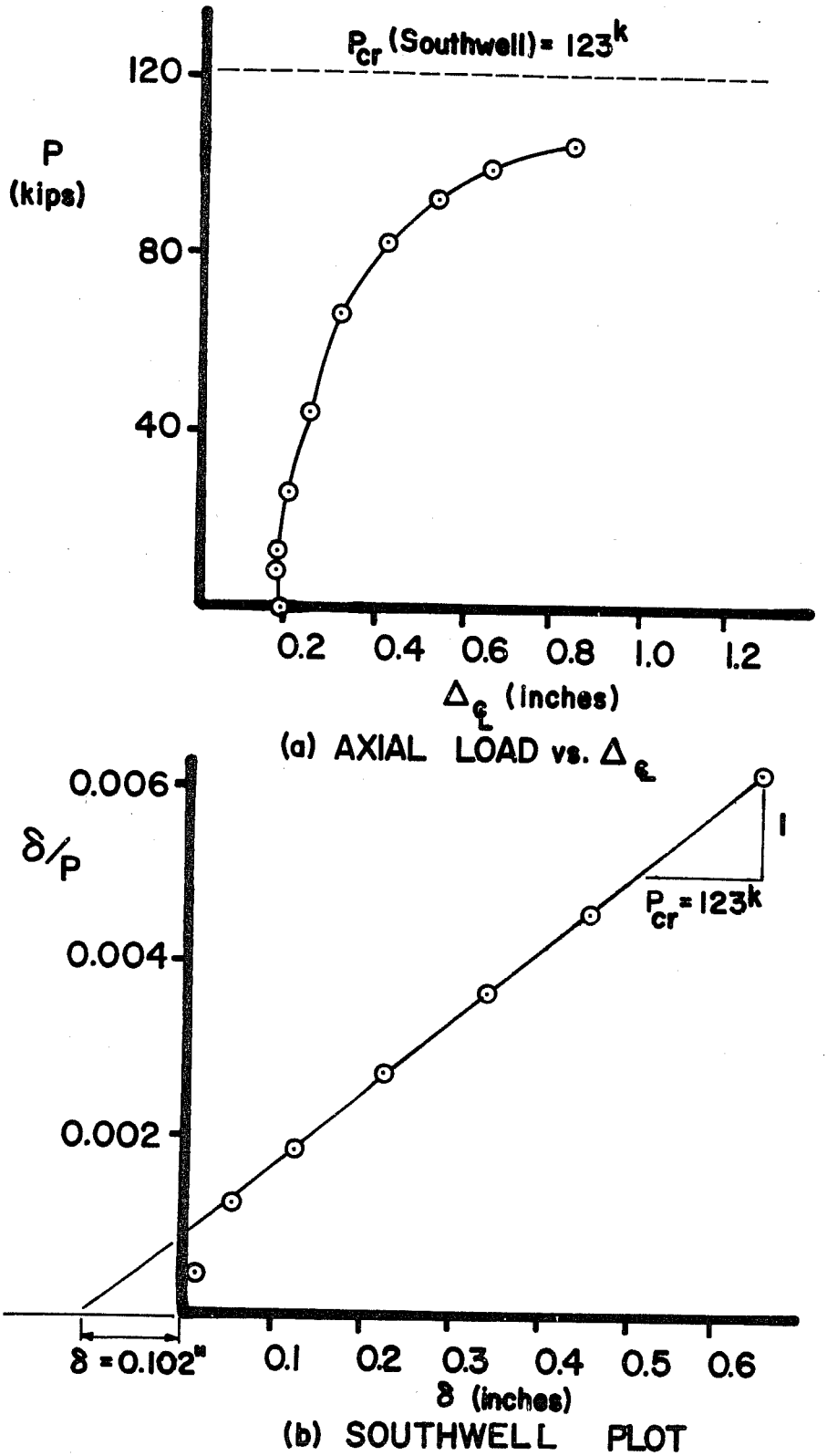

Fig. 3.4 Column behavior--Test I

be near zero, since the slope of the curve is near zero. As can be seen in Table 3.1, the values of the initial beam moments prior to column loading, M_{ow}/M_p and M_{oe}/M_p, are 0.078 and 0.079, respectively. The small (1 percent) difference between these values, coupled with the general agreement in the shapes of the curves, indicates that all four joints are approximately the same strength.

The moment-rotation history of each joint during column loading is also shown in the figures. During the column loading, the column deflected eastward and the beam end supports were locked in position. This caused the east beams to load while the west beam joints unloaded. As seen in Fig. 3.2, the additional loading portion of the curves for the east beams is flat, yielding a stiffness of zero and providing no additional restraint to the column. The west beams, however (Fig. 3.3), were unloading along a line with a slope of about one-half (46 percent) of the elastic stiffness line's slope. This indicates that some restraint is being provided to the column by the west beams.

Column behavior for Test I is represented by the curves in Fig. 3.4 and the pertinent values are listed in Table 3.1. The Southwell buckling load was determined from the last five data points to be 123 kips. By changing the first and last data points of this series by the degree of reliability of the data ($4\mu\epsilon$ for loads and 0.004 in. for deflections) and computing values of P_{cr} from lines joining these points, a range of buckling loads was found to be 121 to 125 kips. This range indicates that P_{cr} is reliable to within 2 percent. Figure 3.4(a) shows a trend which is also apparent for the plots of P versus Δ_{ℓ} for the remaining tests; i.e., at low levels of axial load column centerline deflections are small but are seen to increase rapidly as the Southwell buckling load is approached. The maximum column load was 87 percent of the Southwell buckling load and was considered adequate to predict the active buckling load. Column loading was terminated at this load,

because it was determined that yielding was imminent and the Southwell plot was satisfactory.

3.3 Results of Test II

The results of Test II are included in Table 3.1 and Figs. 3.5 through 3.7. In this test the connecting angle was bolted to the beam web and welded to the column web, as shown in Fig. 2.3(b). The plots in Figs. 3.5 and 3.6 illustrate the beams' behavior during the test. The vertical scale (M/M_p) in these figures is greatly expanded from the previous plots for Test I, because the connections used (Connection B) were less stiff than those used in Test I. Throughout the loading of the beams to the desired rotation and moment level, M_o, the connections exhibited a generally linear moment-rotation relationship. Small deviations from this line could be attributed to unequal frictions in the setup and experimental error. Since the magnitude of the loads, and therefore moments, was relative small, these factors had more effect in this test than in the others. Three of the beams exhibited the same elastic stiffness, while the southeast beam appeared to be less stiff than the others. Upon careful consideration of the data, the only reasons apparent for this difference are those stated above. During column loading, the east beams continued to load, as in Test I, along a relatively flat slope. The inconsistent nature of the loading curve for the east beams must be attributed to the reliability of load readings illustrated in Fig. 3.5. A 4$\mu\epsilon$ difference in the beam load cell readings gives a difference in $M/M_p = 0.002$. Since the plots of the east beams show no additional restraint available for the column, the reduced elastic stiffness of the southeast beam was not considered to be important. Since the values of initial beam moments for the west and east beams, 0.0253 and 0.0252, are in close agreement, and the general shape of the curves is so similar, all four joints are considered as having the same strength. As stated and shown in Fig. 3.5, during the

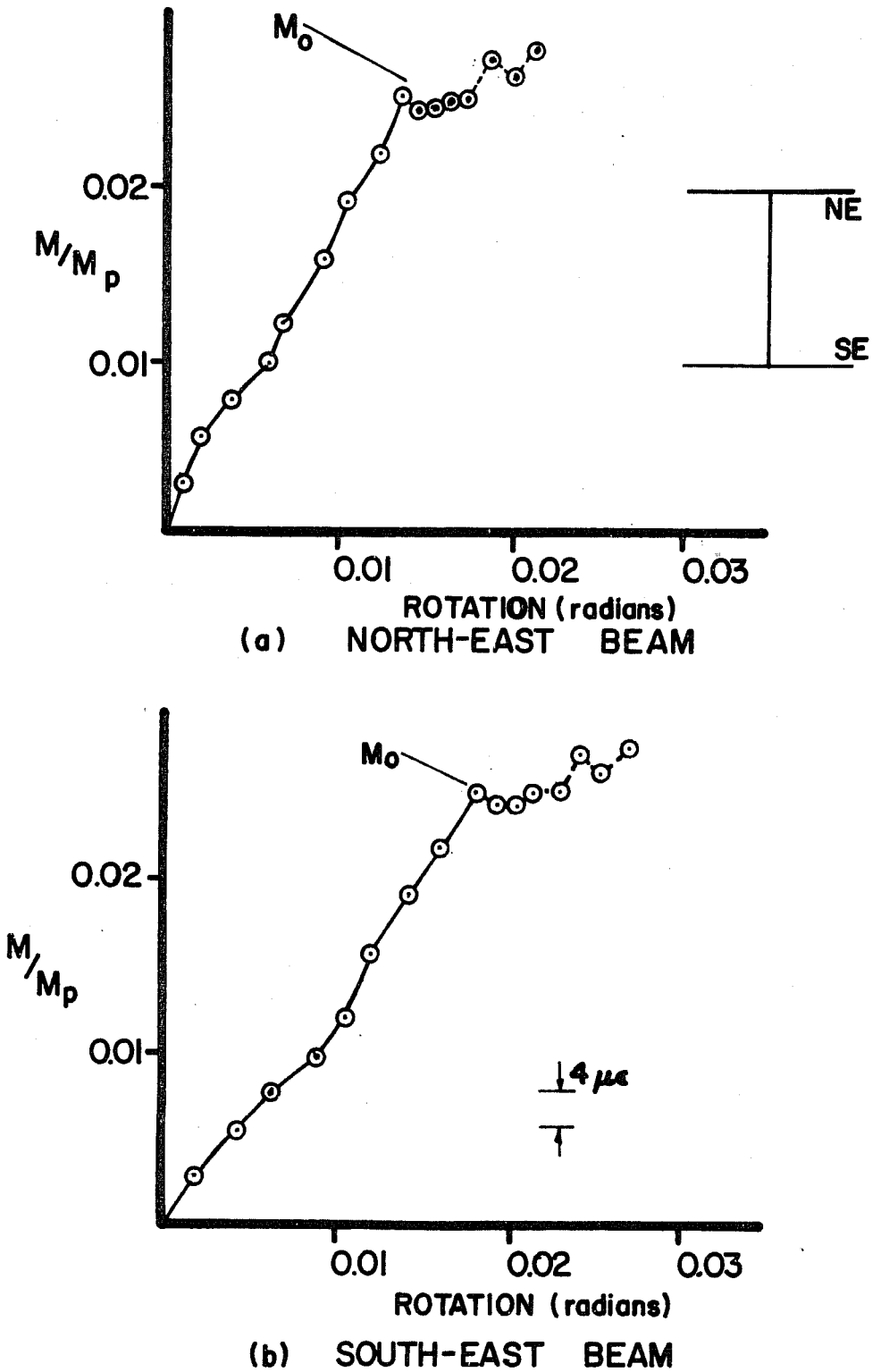

Fig. 3.5 Beam behavior--Test II

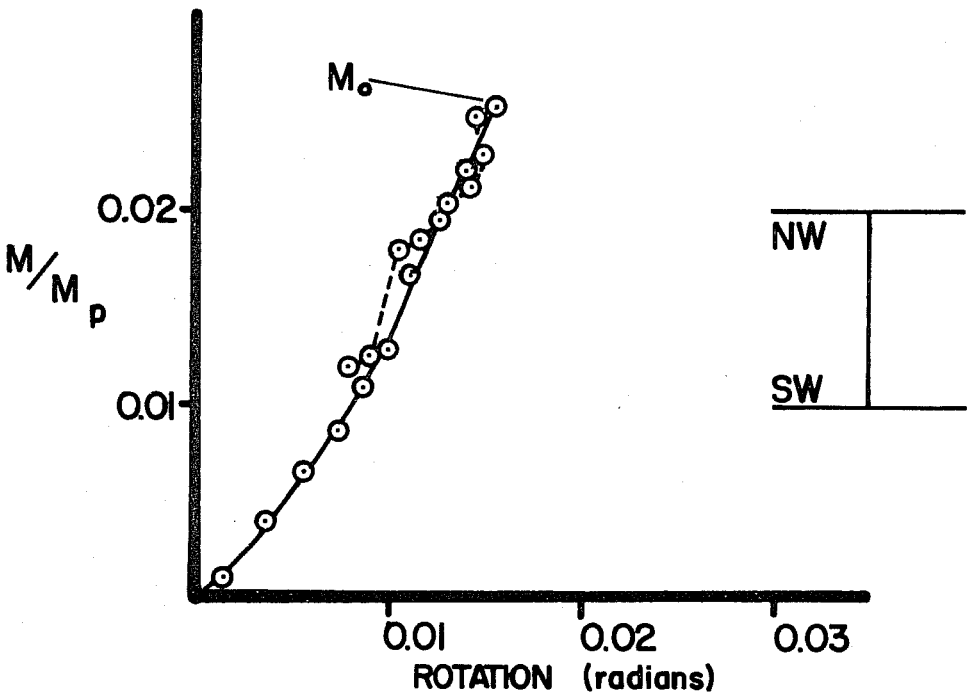

(a) NORTH-WEST BEAM

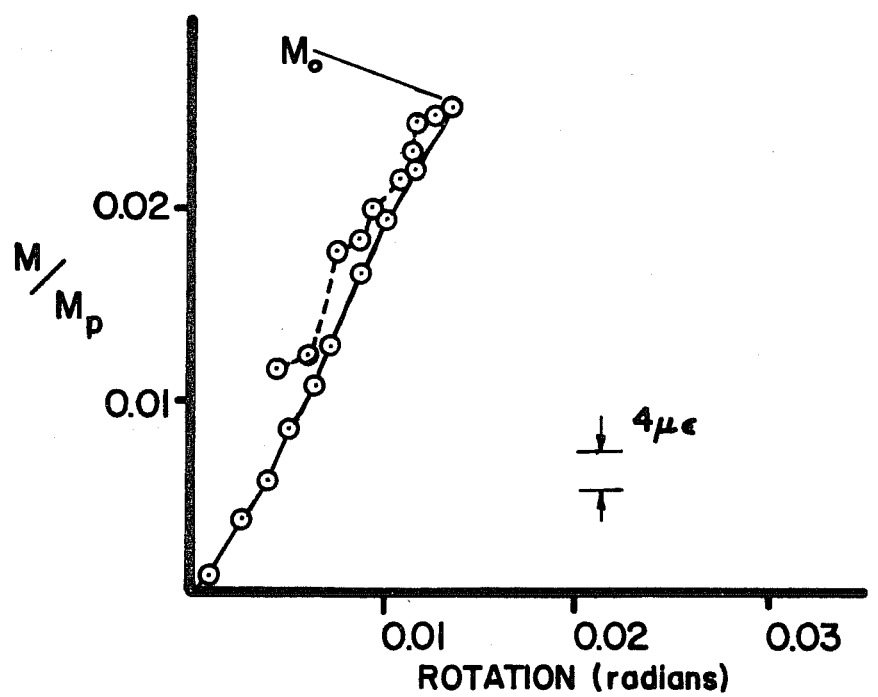

(b) SOUTH-WEST BEAM

Fig. 3.6 Beam behavior--Test II

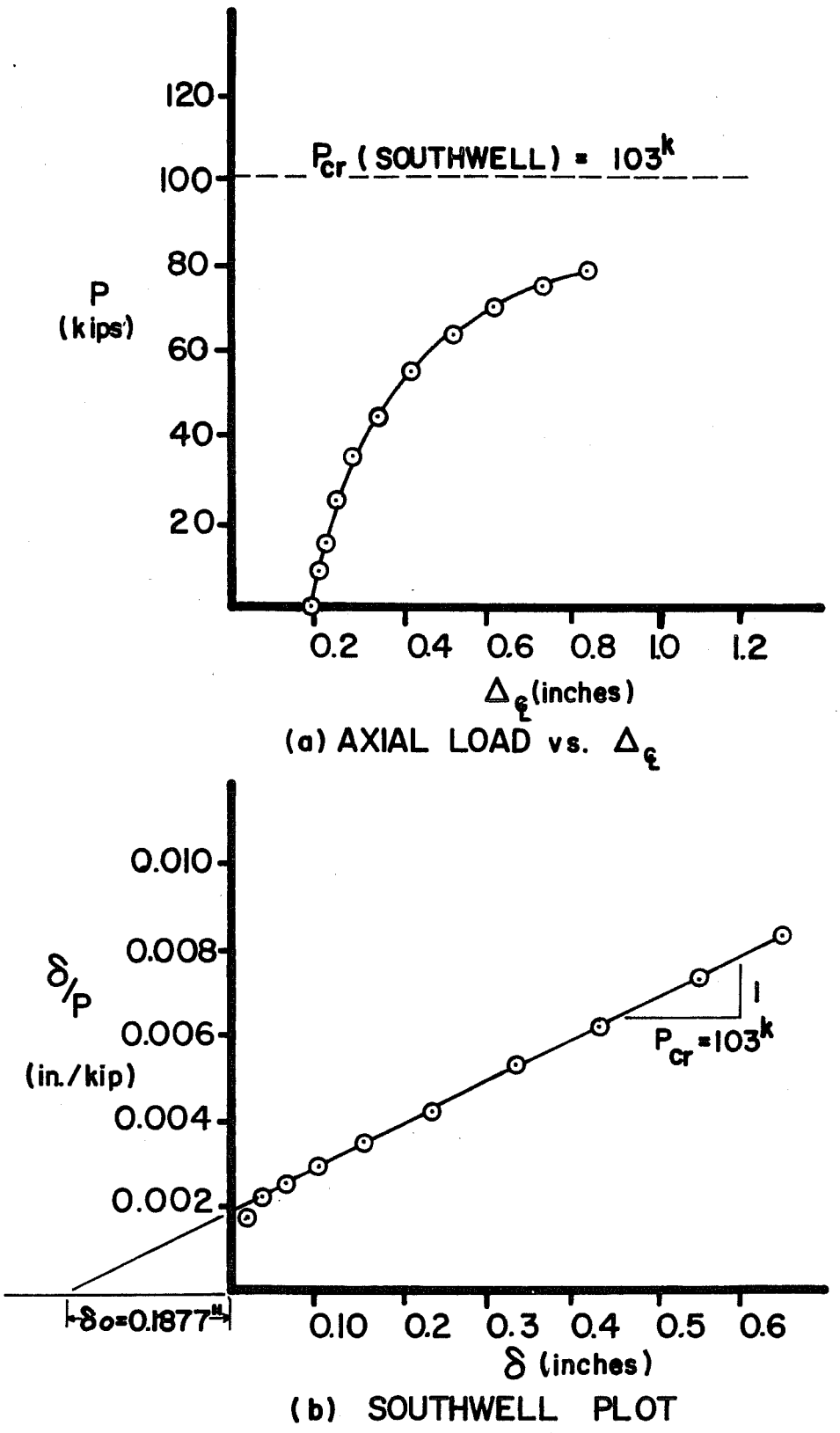

Fig. 3.7 Column behavior--Test II

column loading the east beams offered no additional rotational restraint to the column. However, during this sequence, the west beams were unloading, as shown in Fig. 3.6. The slope of the unloading portion of the curve is approximately the same as the loading curve, indicating that the west beams offer restraint equal to the elastic stiffness.

Column behavior for Test II is shown in the plots in Fig. 3.7 and the results are listed in Table 3.1. The buckling load determined from the Southwell plot was 103 kips. Figure 3.7(a) shows the load-deformation characteristics of the column with small deflections at low load levels and increasing deflections as the buckling load is approached. The maximum column load was 78 percent of the Southwell buckling load and was considered adequate to predict the actual buckling load.

3.4 Results of Test III

The results of Test III are included in Table 3.1 and Figs. 3.8 through 3.10. The connecting angle for this test was bolted to the column web and welded to the beam web (Connection C), and is shown in Fig. 2.3(c). The curves in Figs. 3.8 and 3.9 show the beams' behavior. The general shape of the curves up to M_o is similar to those of Test I; that is, initially the shape is linear of a slope equal to the elastic stiffness, then deterioration of the stiffness until the curve flattens to a stiffness near zero. From the table it can be seen that the imbalance of moments on either side of the column is again small, 0.0676 on the west and 0.0685 on the east (1 percent difference), and the general shapes of the curves are similar. The northeast beam, however, seems to have a higher elastic stiffness than the rest, but it is again on the loading side of the joint, and the elastic stiffness will not affect the results. This increased stiffness was probably due to uneven frictions in the test setup. During column loading, the

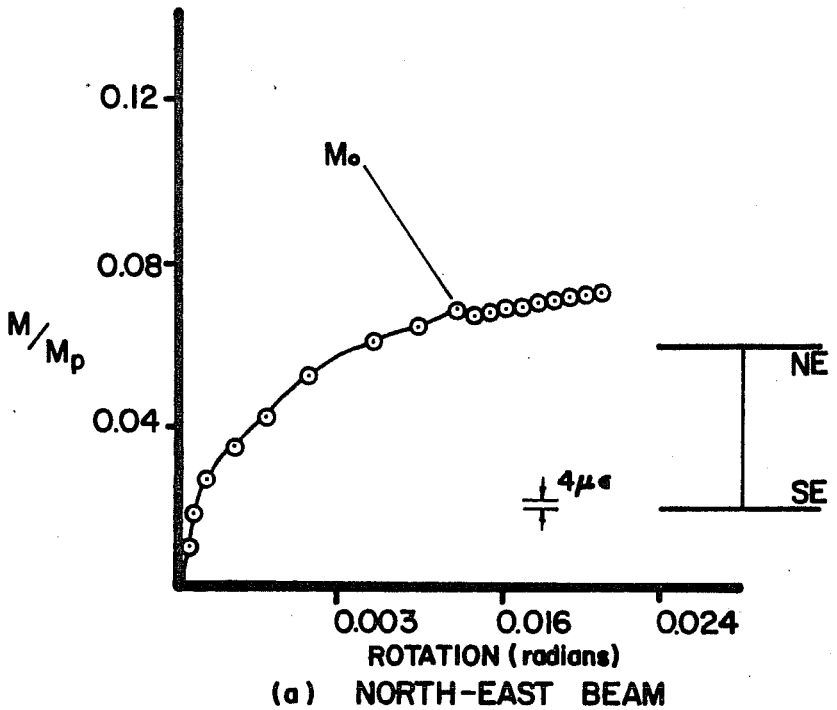

(a) NORTH-EAST BEAM

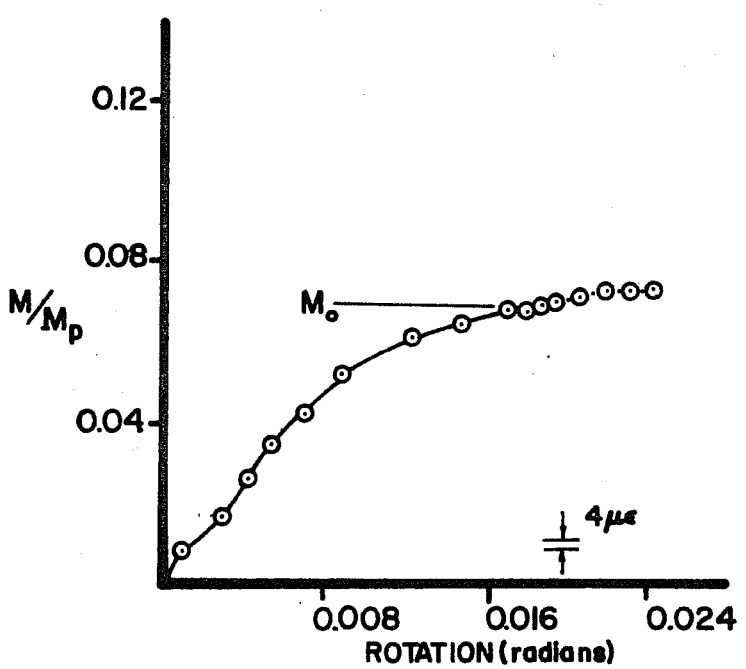

(b) SOUTH-EAST BEAM

Fig. 3.8 Beam behavior--Test III

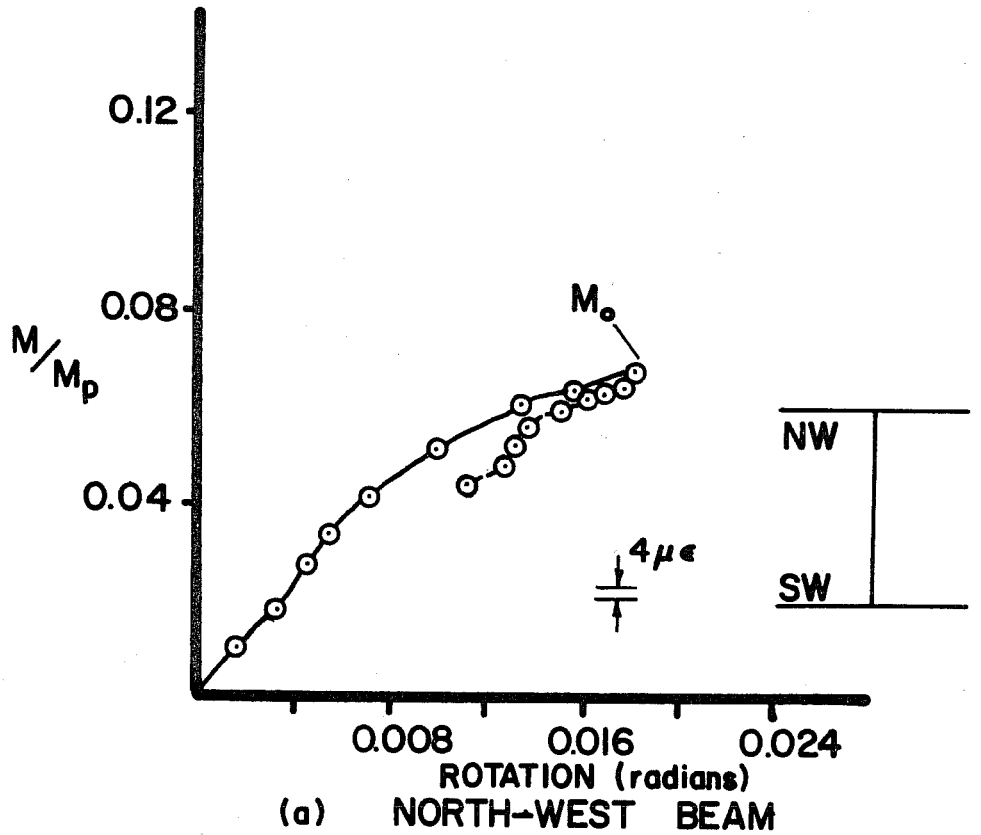

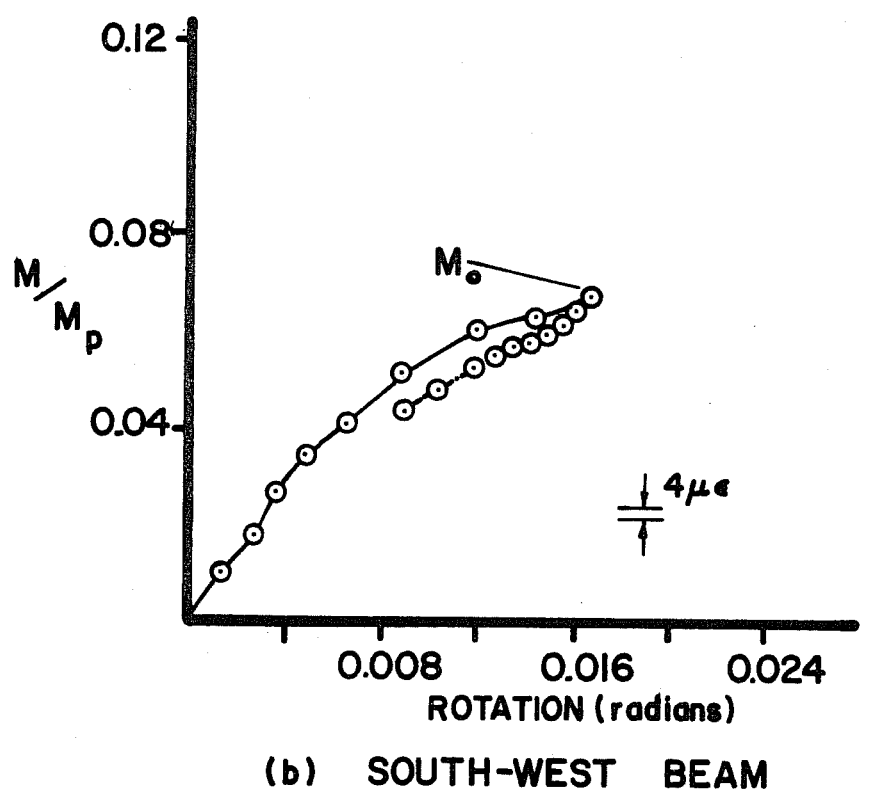

Fig. 3.9 Beam behavior--Test III

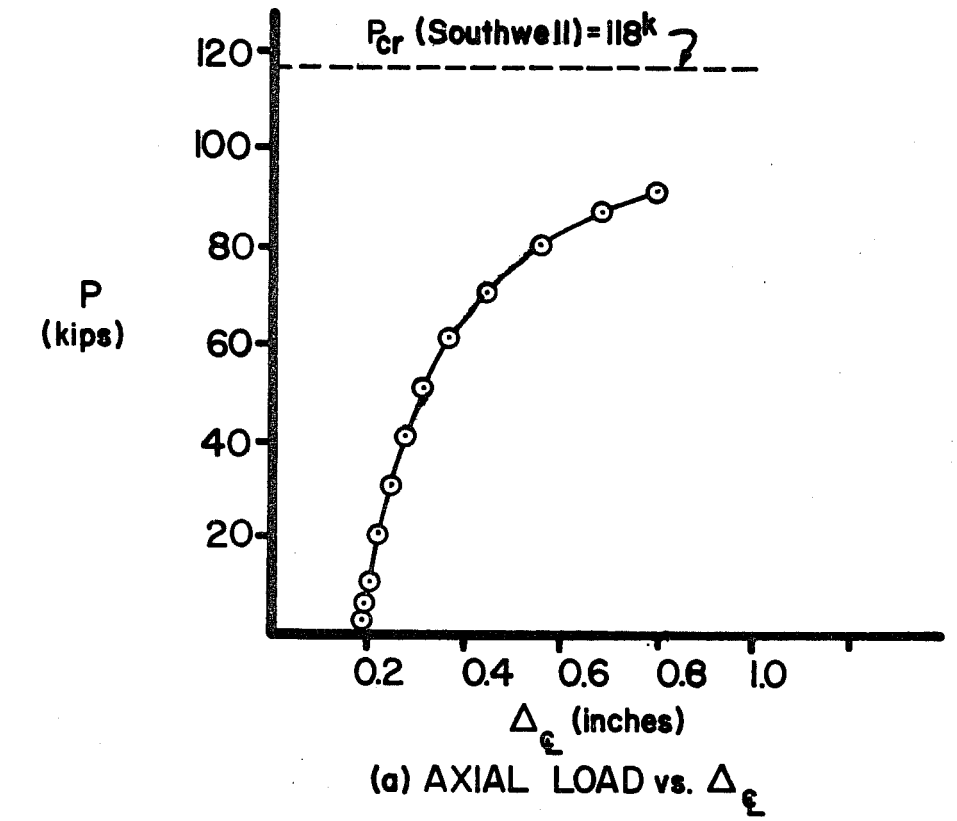

(a) AXIAL LOAD vs. Δ_{ℓ}

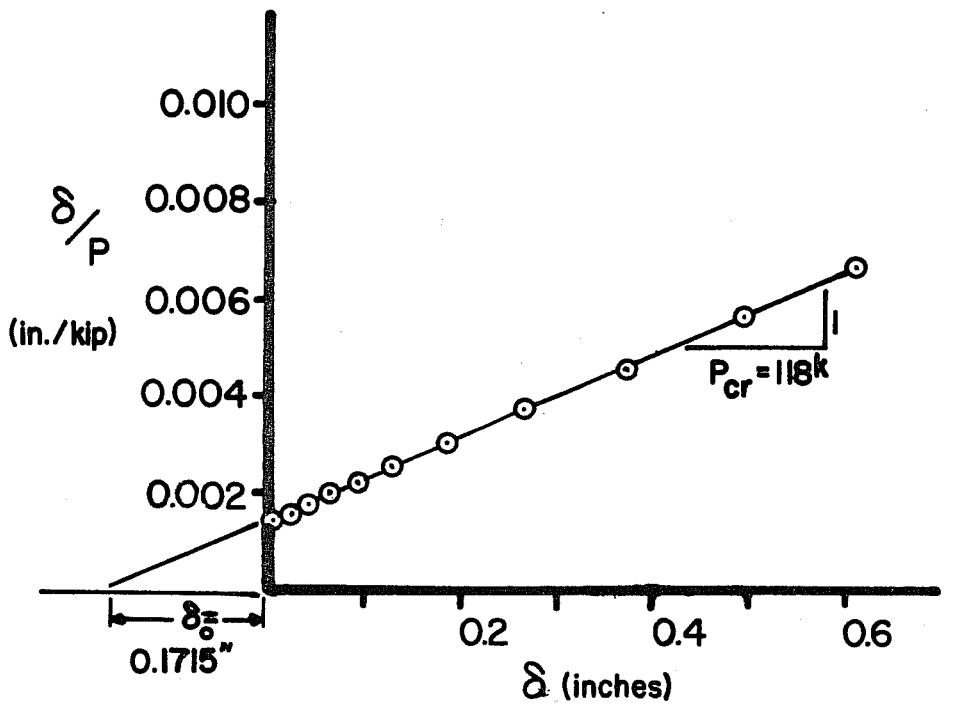

(b) SOUTH WELL PLOT

Fig. 3.10 Column behavior--Test III

east beams again loaded on a flat slope and offered little or no restraint, while the west beams unloaded with a stiffness of about half (40 percent) of the elastic stiffness. As is shown on the plot, the sensitivity of the data acquisition system could account for slight variations in the loading and unloading curves.

Figure 3.10 shows plots of column behavior for Test III, and the last five points of the Southwell plot were used to compute the buckling load of 118 kips. The maximum load reached, P_{max}, is listed in Table 3.1 as 91.8 kips, and was 78 percent of the Southwell buckling load. This was considered adequate and the column loading was stopped in order to ensure elastic action.

3.5 Results of Test IV

The connection used in this restrained beam-column test was the same as that used in Test I, an all bolted connection. The curves in Figs. 3.11 through 3.13 show the behavior of the beams. The general shape of the curves up to the M_o level are very similar to those of Test I. The elastic stiffness of the west beams is higher than that of the east beams. This was noted during the test and auxiliary supports were placed under the west beams to release the frictions that were thought to be the cause of this difference. The effect of this can be seen in the slight change in the curves at an $M/M_p = 0.068$. Although there was a difference in elastic stiffnesses, the moment levels on either side of the joint were exactly the same at the end of beam loading, M_o.

The characteristics of the joints that continued to load as the column was subjected first to axial load and then lateral load are shown in Fig. 3.11. The loading curve was very flat with very slight variations showing that no additional stiffness is offered by these beams. The responses of the unloading beams, shown in Figs. 3.12 and 3.13, exhibit reasonably the same behavior. The initial unloading is linear with a slope of about 47 percent of the

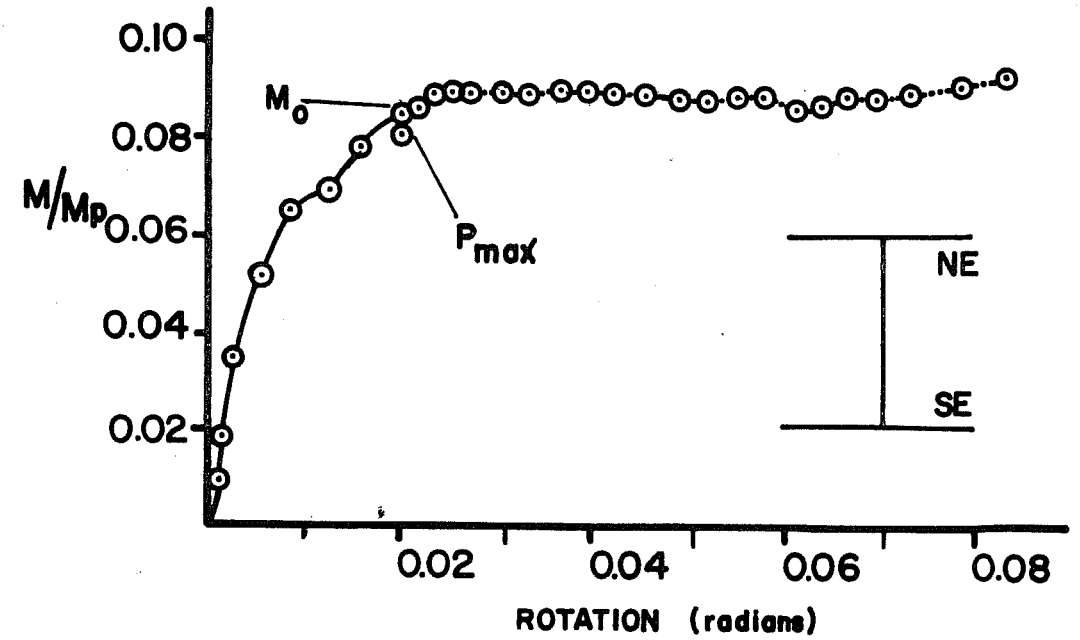

(a) NORTH-EAST BEAM

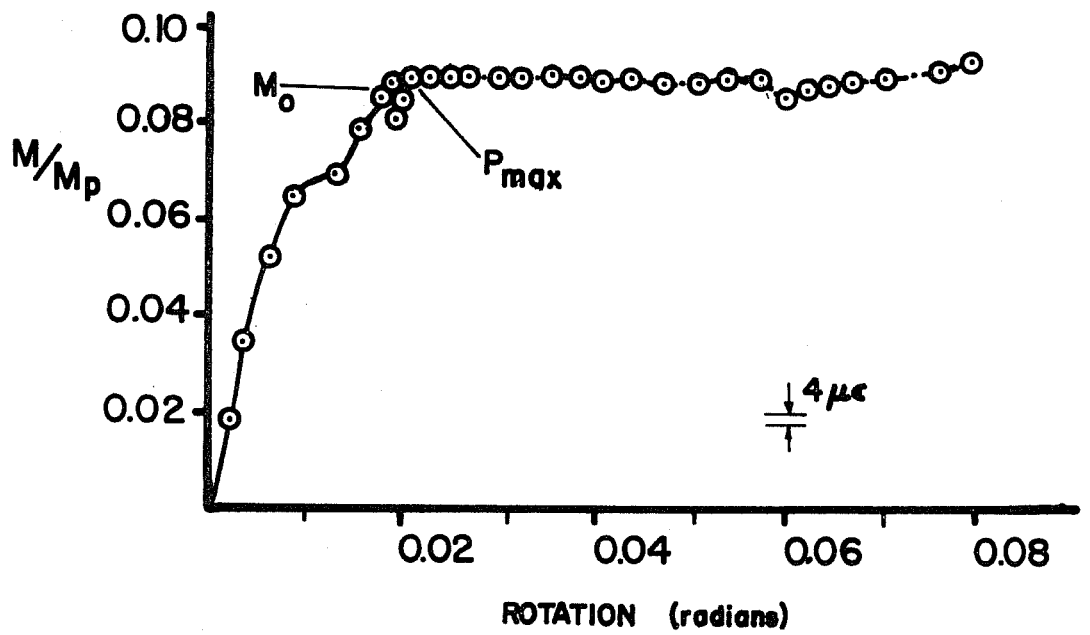

(b) SOUTH-EAST BEAM

Fig. 3.11 Beam behavior--Test IV

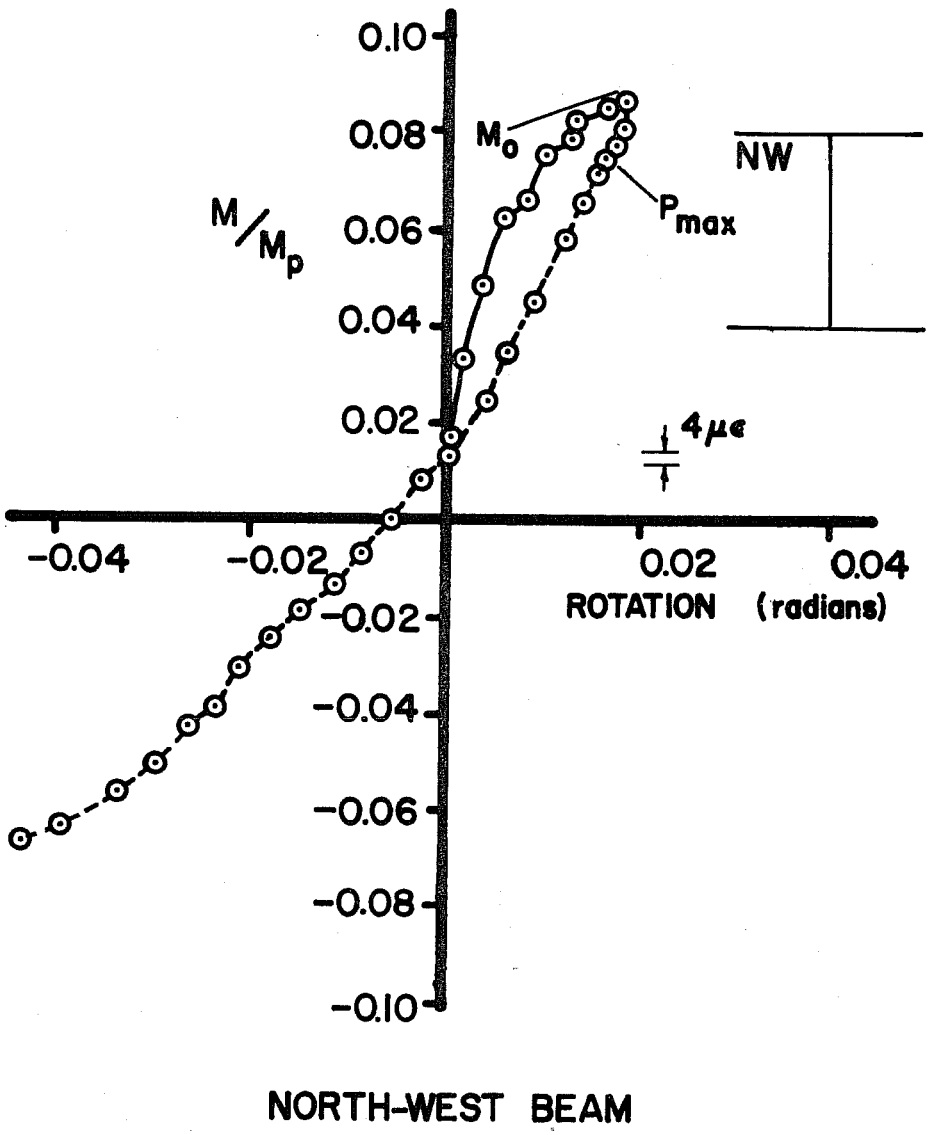

Fig. 3.12 Beam behavior--Test IV

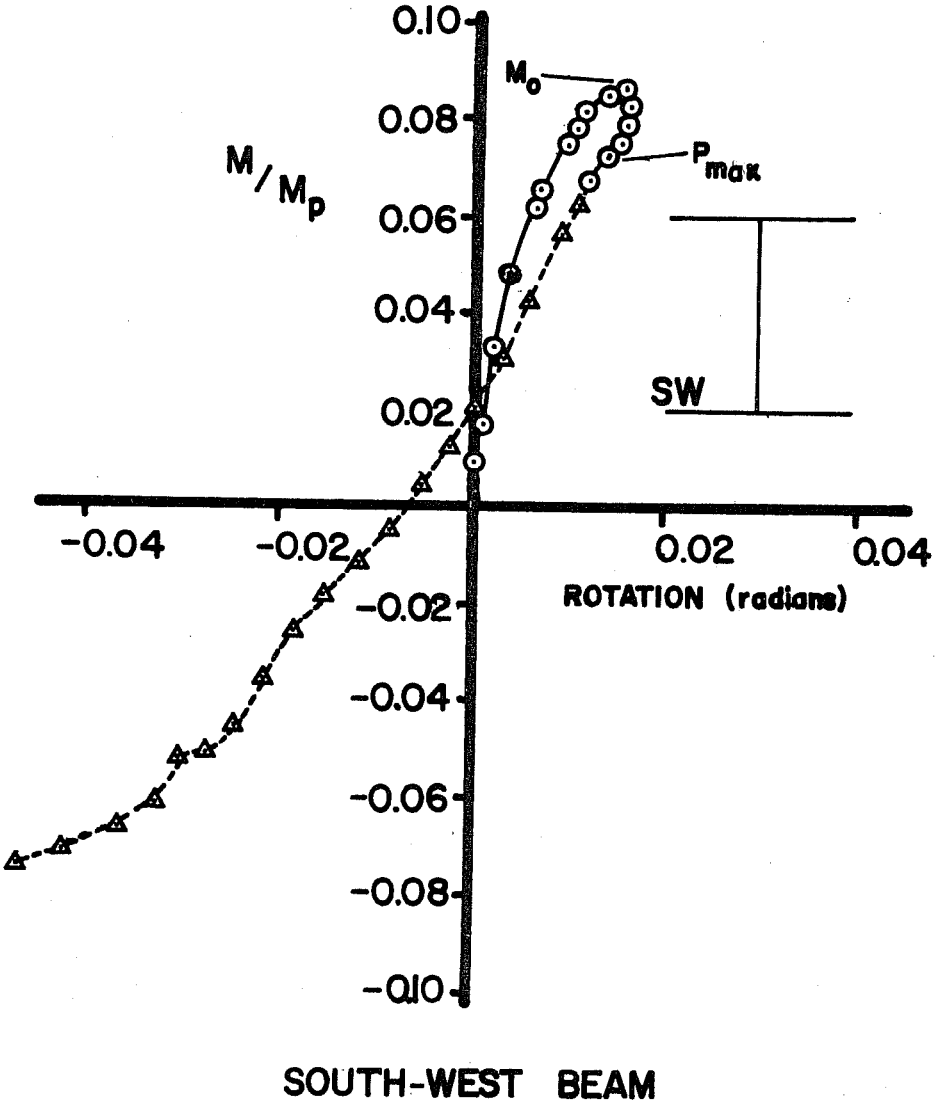

Fig. 3.13 Beam behavior--Test IV

elastic stiffness. Once the rotations have reversed though, the unloading is linear with a slope of about 25 percent of the elastic stiffness. As shown on the plots, the error incurred in obtaining data is of sufficient magnitude that it could account for the slight variations in the curves, especially the loading and unloading curves. Since there was no pumping of load into the beam system, the strain indicator error of 4με is significant.

Figure 3.14 shows plots of the column behavior up to the level of axial load held during the lateral loading. Also, these plots show the column behavior from Test I for the same range of load. Although the load level was not sufficient to predict a buckling load from the Southwell plot (42 percent of P_{cr}), the curves show the general agreement between the column behavior of the two tests. This observation, coupled with the similarities of the beam curves for the two tests, indicates that this specimen with the same type of connection would have very nearly the same buckling load as that of Test I, P_{cr} = 123 kips.

Column behavior during application of lateral load is represented in a plot of lateral load versus column centerline deflection, Fig. 3.15. The curve is generally linear up to about 1.5 kips, then a gradual deterioration of stiffness occurs until instability is encountered. No further data were recorded because of the large centerline deflection (6 in.). At a load of about 3.25 kips, a slight shift of the curve is noted. At this stage in the test it was noted that one of the screw jacks used for alignment of the column was in contact with the column and was possibly absorbing some lateral load. Upon release of the jack, the load did go down and this shows in the curve; but, as can be seen in the curve, the slopes of the lines before and after this shift are about the same (5 percent difference), so this shift was not

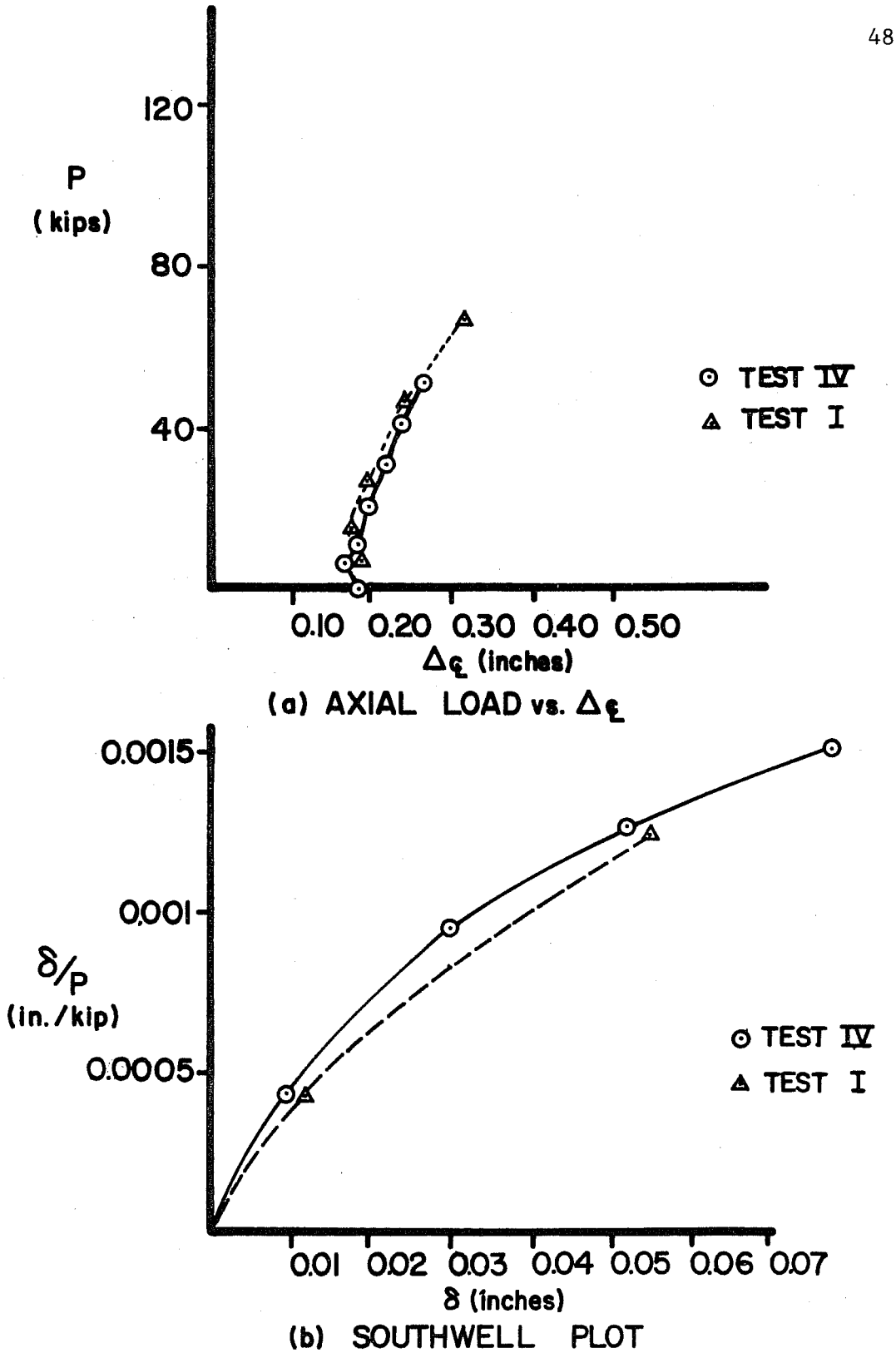

Fig. 3.14 Column behavior--Test IV, axial load

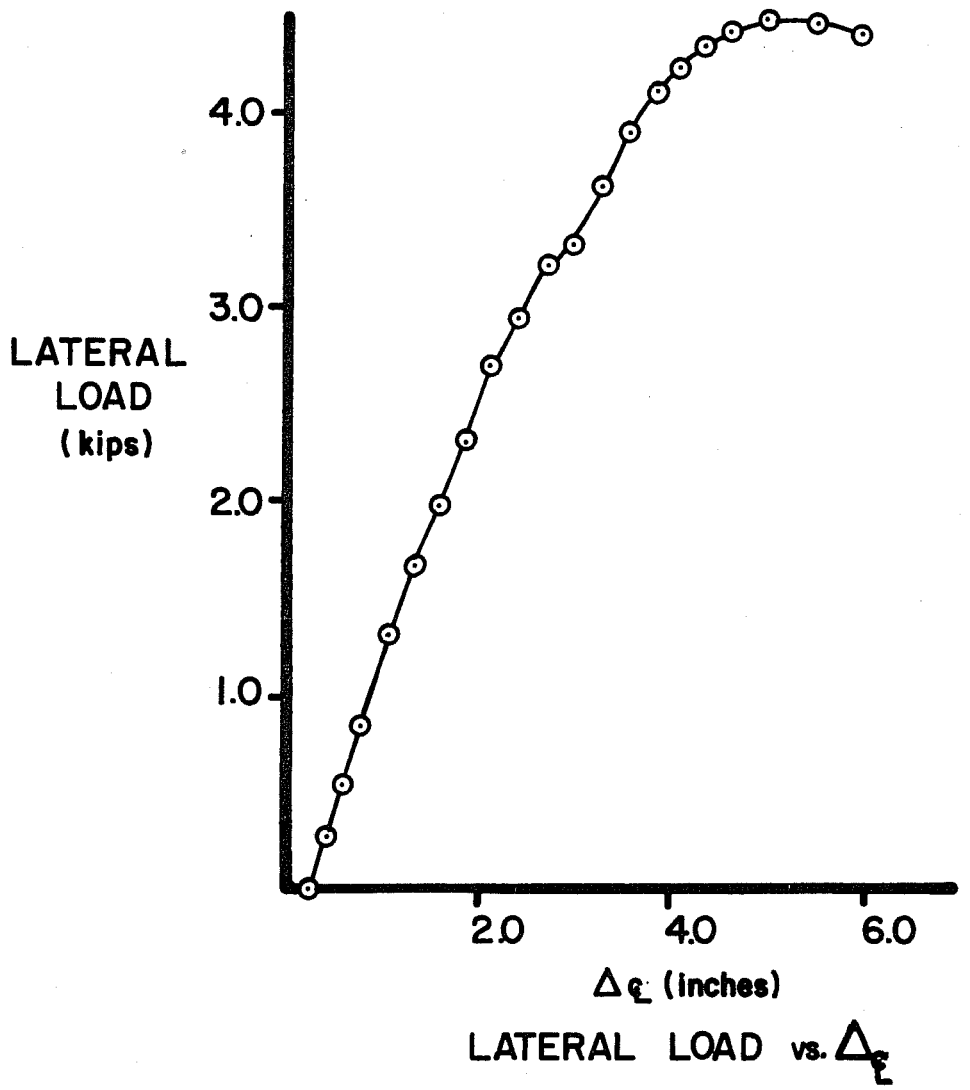

Fig. 3.15 Column behavior--Test IV, lateral load

important. The maximum lateral load of 4.49 kips occurred at a centerline deflection of 5 in. (Fig. 3.15).

CHAPTER 4

DISCUSSION OF TEST RESULTS

4.1 Joint Stiffnesses

Table 4.1 summarizes the flexibility factors of the three connection types used in the test program. The table includes the elastic and unloading flexibility factors from the M-θ test series and the four major experiments. Also included are the flexibility factors recommended by DeFalco and Marino,[4] and Peterson and Cermak.[7] A comparison of the elastic flexibility factors from the experiments shows that connection types A and C, which were bolted to the column, exhibited reasonably similar behavior. This similarity can be attributed to the fact that the distance from the heel of the angle to the column web bolt is similar for Connections A and C (see Fig. 2.3). Connection C is more flexible (33 percent) than Connection A, due to the increased distance to the beam web connectors, but it is obvious that the distance to the column web connection is the most critical variable affecting joint flexibility. Connection B, however, is approximately four times more flexible than Connections A and C, since the distance to the column web connector, the weld, is much greater (3-1/2 in. versus 2-5/8 in.), which causes a reduction in rotational stiffness. This trend is also apparent in the elastic flexibility factors obtained from Peterson and Cermak.

As stated earlier, the connections on one side of the column continued to load during the column loading stages, while those on the other side unloaded. The loading connections deformed plastically with zero stiffness, while the others unloaded linearly,

TABLE 4.1 CONNECTION FLEXIBILITY FACTORS

Connection Type	Test	Z_{test} (rad/kip-in.)		Z*	Z
		Elastic	Unload	Marino	Peterson & Cermak
A	I	1.0×10^{-4}	2.8×10^{-4}	0.31×10^{-4}	$1.7^{**}\times10^{-4}$
	IV	0.9×10^{-4}	2.9×10^{-4}	0.31×10^{-4}	1.7×10^{-4}
	M-θ (1)	0.94×10^{-4}	1.1×10^{-4}	0.31×10^{-4}	1.7×10^{-4}
B	II	6.1×10^{-4}	6.1×10^{-4}	0.31×10^{-4}	3.8×10^{-4}
	M-θ (2)	5.7×10^{-4}	5.2×10^{-4}	0.31×10^{-4}	3.8×10^{-4}
C	III	1.5×10^{-4}	3.0×10^{-4}	0.31×10^{-4}	1.8×10^{-4}
	M-θ (3)	1.4×10^{-4}	1.4×10^{-4}	0.31×10^{-4}	1.8×10^{-4}

*Based on 7/16 in. angle thickness; test thickness was 1/4 in.

**Example calculation presented in Appendix C.

defined as the unloading stiffness. As would be expected, the differences between the unloading stiffnesses for the connections was the same as the differences between the elastic stiffnesses. For Connection B the unloading and elastic stiffnesses were the same. However, in the column tests using Connections A and C, the unloading behavior of the connections was considerably more flexible than the initial elastic response. Since the unloading stiffness is what is present during column buckling, it should be used in stability calculations for the column. Also, since the loading connections exhibit no stiffness, only one beam should be considered for column restraint in the buckling calculations.

A comparison of the elastic flexibility of the joints from the four tests with those from the M-θ tests shows that the M-θ tests exhibit slightly higher stiffnesses (Connection A, 10 percent; Connection B, 6.5 percent, and Connection C, 7 percent). Also, the unloading stiffnesses are much closer to the elastic stiffnesses in the M-θ tests; only about a 17 percent reduction in stiffness is noted during unloading for Connection A, while no reduction occurred in Connection B. Both of these differences can be attributed to the fact that in the M-θ tests the beam was attached to the flanges of a column while in the major experiments they were connected to the column web. During unloading, the relatively thin column web bends as it resists the forces from the connection angle, as seen in Fig. 4.1. Since the web is very flexible, these web deformations reduce the stiffness of the joint. In column tests I and III, the web deformations reduced the stiffness by 64 percent and 50 percent, respectively. When the beam is connected to the flange of the column, this effect is not as great and the unloading stiffness is about 90 percent of the elastic stiffness.

Lothers[6] has presented a theoretical procedure for calculating a connection's elastic flexibility and refinements on this procedure were discussed by Peterson and Cermak.[7] DeFalco and

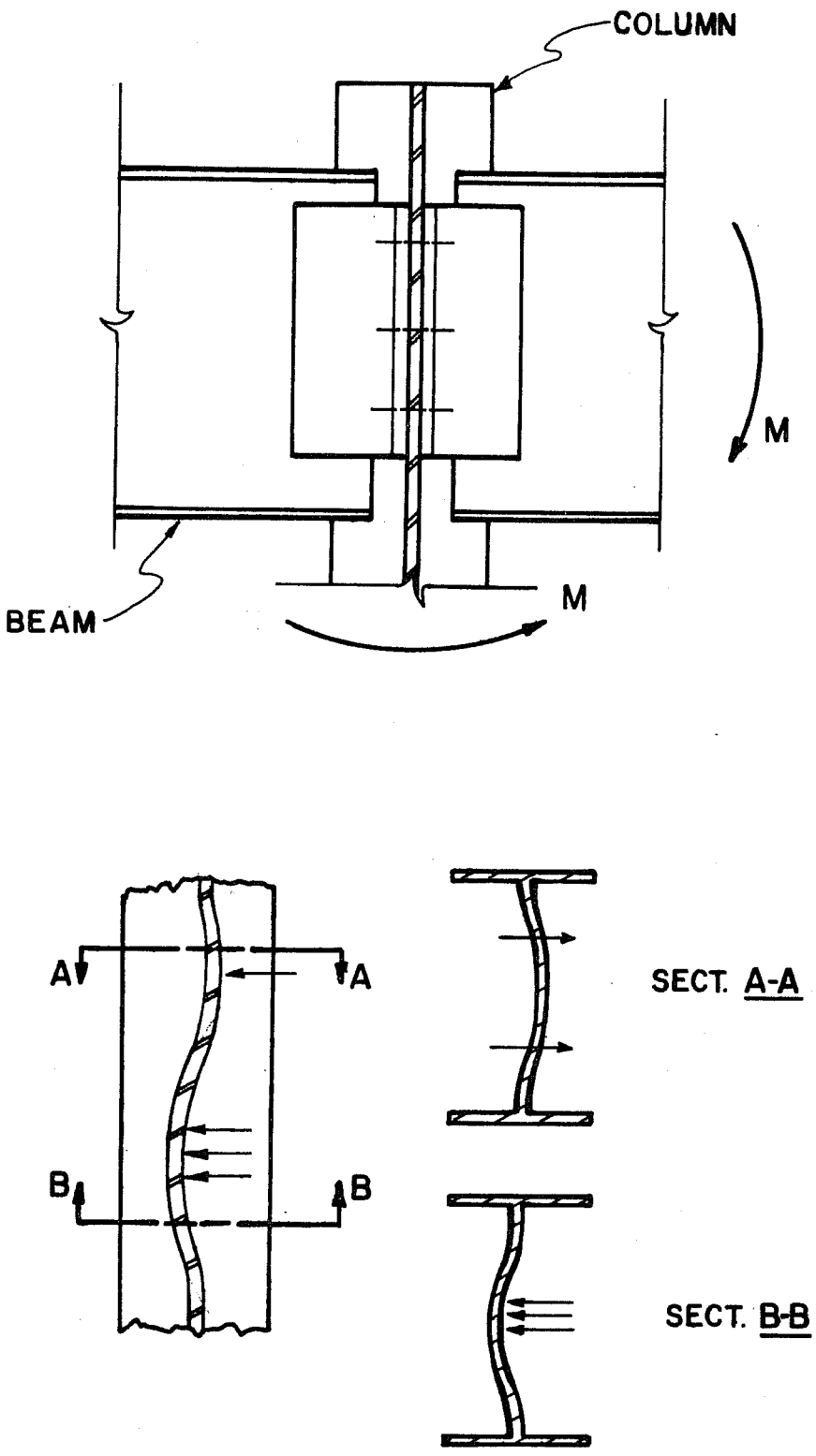

Fig. 4.1 Column web deformation

Marino present tables of flexibility factors for various connections, and the values for connection types A, B, and C are listed in Table 4.1. The DeFalco values were obtained using Lother's procedure, and it is believed that an angle thickness of about 7/16 in. was used. The greater thickness accounts for the reduced flexibility. When using angle thicknesses different from the standard AISC thicknesses for Type II connections. Peterson's method should be used in lieu of DeFalco's tables in the determination of flexibility factors. For Connections A and C, Peterson and Cermak's equations underestimate the stiffness by approximately 32 percent, but the stiffness for Connection B is overestimated by 61 percent. The difference for Connection B probably stems from the fact that in the development of the equations Lothers assumes that the leg of the connection angle is fixed against rotation at the connector location, while in the test this point is welded and rotation was observed during loading.

The differences between the theoretical values for joint stiffnesses and the test values appear to be great. The effect of these differences on overall column stability will be evaluated in the following section.

4.2 Theoretical Buckling Analysis

A theoretical buckling analysis was performed on each specimen in which the far ends of the restraining beams were assumed to be perfectly pinned to simulate the actual test conditions, as shown in Fig. 2.1. The fact that the column axial load was applied 11 in. above the intersection of the beam and column was considered, along with the effect of the semi-rigid connections.

In order to find an expression for the buckling load of the test assemblage, the structure was modeled as shown in Fig. 4.2(a). In this structure only one beam at each joint is assumed to restrain the column due to the nature of the beam loading discussed earlier;

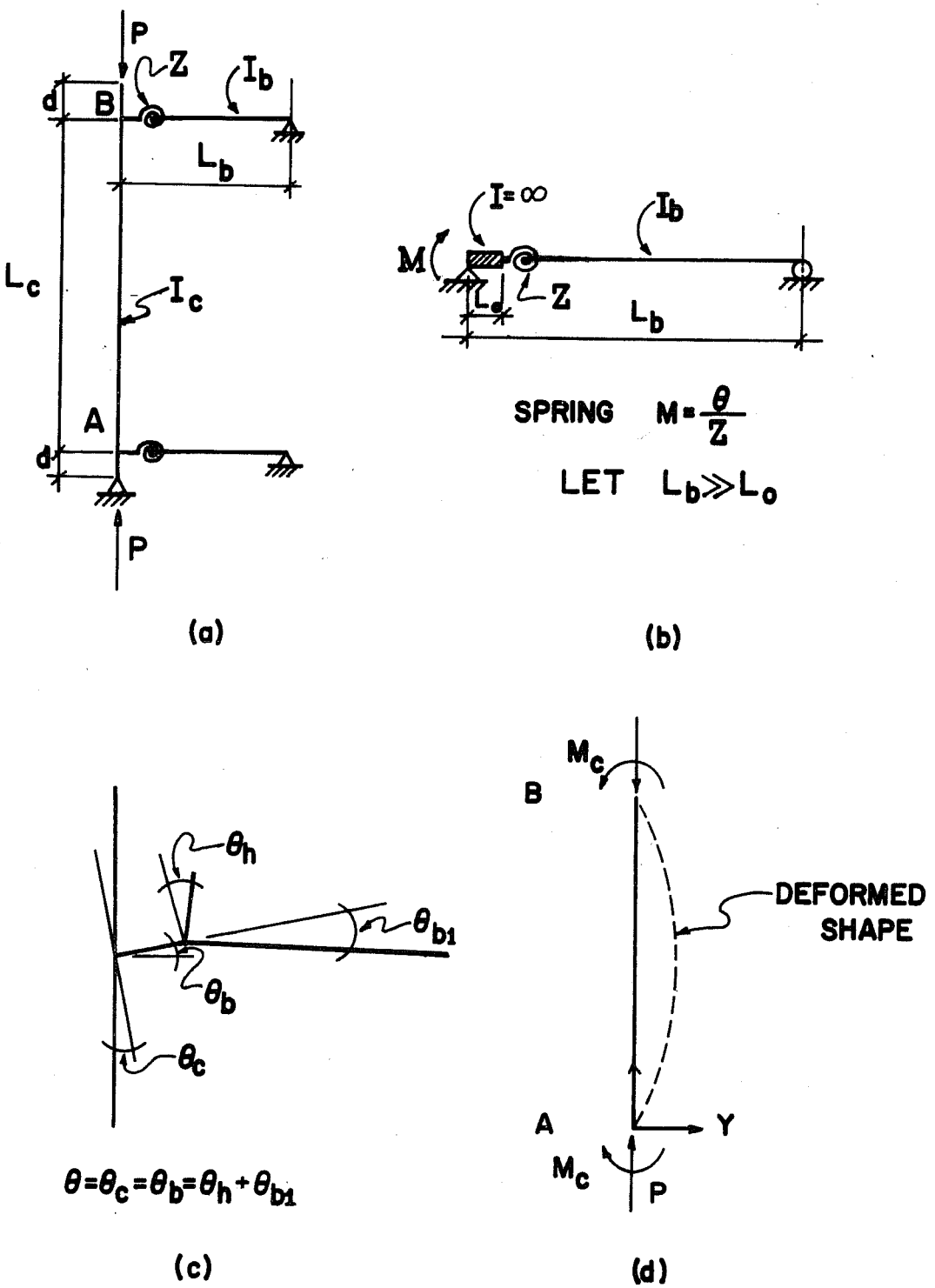

Fig. 4.2 Theoretical analysis

namely, the fact that the connections on one side of the column exhibit zero stiffness during column buckling. The column axial load is applied at a distance, d, away from the center of the beam to column joint.

First, to arrive at an expression for the angle change at the end of the beam due to an applied moment, the beam was modeled as shown in Fig. 4.2(b), with simple supports and two members joined by a spring which represents the semi-rigid connection. One member is relatively rigid and the other has the properties of the beam.

By applying conjugate beam methods and treating the spring as a concentrated angle change equal to $\theta_h = M \cdot Z$, an expression for the slope at the left end is:

$$\theta_b = \frac{M_b Z \, L_b}{L_b - L_o} + \frac{\frac{M_b}{EI_b} \cdot \frac{L_b}{2} \cdot \frac{2L_b}{3}}{L_b - L_o}$$

As L_o approaches zero, the expression becomes

$$\theta_b = M_b Z + \frac{M_b L_b}{3EI_b} = M_b [Z + L_b/3EI_b] \qquad (4.1)$$

where the term in brackets is the inverse of the beam stiffness.

Taking a free-body diagram of the column, considering symmetry as shown in Fig. 4.2(d), the equation of bending is

$$Y'' = -M/EI,$$

and $$M = PY + M_c.$$

Letting $$k^2 = P/EI,$$

then $$Y'' + k^2 Y = -M_c/EI_c$$

or $$Y''' + k^2 Y' = 0 \qquad (4.2)$$

The solution to Eq. (4.2) is

$$Y = A \sin kx + B \cos kx + C.$$

From the boundary condition

$$Y = 0 \text{ at } x = 0 \qquad B = -C$$

and $EIY'' = -M_c$ at $x = 0$ $\quad B = M_c/P$.

From symmetry

$$Y' = 0 \text{ at } x = L_c/2 \text{ and } A = \frac{M_c}{P} \tan \frac{kL_c}{2} .$$

So the equation for the deflected shape is:

$$Y = \frac{M_c}{P} \tan \frac{kL_c}{2} \sin kx + \frac{M_c}{P} \cos kx - \frac{M_c}{P} ,$$

and

$$Y' \text{ at } x = 0 \text{ equals } \theta_c = \frac{M_c}{P} k \tan \frac{kL_c}{2} . \tag{4.3}$$

Satisfying compatibility, $\theta_c = \theta_b$ (4.4)

and equilibrium, $M_c + M_b + P\theta_c d = 0$, (4.5)

and combining Eq. (4.1), (4.3), (4.4), and (4.5) gives

$$\tan \frac{kL_c}{2} = \frac{kL_c}{2}\left[\frac{2d}{L_c} \cdot \frac{kL_c}{2} \tan \frac{kL_c}{2} - 1\right]\left[\frac{3EI_b}{L_b} Z + 1\right]\left[\frac{2}{3} \frac{I_c/L_c}{I_b/L_b}\right] \tag{4.6}$$

Equation (4.6) for the buckling load takes into account both the "stub" column (the first bracketed term) and the semi-rigid connection (the second bracketed term). The third bracketed term is recognized as the G factor used in determining k for the column from the alignment chart. The constant 2/3 factor accounts for the fact that the braced case alignment chart assumes a beam stiffness of 2EI/L (equal rotation at both ends of the beam) in its development and the beam stiffness for this solution (far end pinned) was 3EI/L.

By substituting in the actual values of d, Z, I_b, L_b, I_c, and L_c from the tests into Eq. (4.6) and solving, the theoretical buckling load for the three stability tests was found. For each solution one beam was considered to give restraint and the

unloading Z was used for each beam. For Test I the theoretical solution gave a buckling load 1 percent higher than the test value, 124 kips versus 123 kips. For Test II, the theory was 3.4 percent below the test, 99.5 kips versus 103 kips; and for Test III the theory was 3 percent above the test value, 122 kips versus 118 kips. These differences are well within the tolerance for experimental error and show that the tests substantiate the theoretical solution using the unloading Z and one restraining beam or joint. Also, by setting d equal to zero in the first bracketed term, and solving the equation, it is possible to determine the effect of the stub on the buckling load. Using this procedure, the effect of the stub was to reduce the buckling load by 12 percent in Test I, 14 percent in Test II, and 12 percent in Test III. A comparison of the buckling load obtained from Eq. (4.6) neglecting the stub effect to the load found using the alignment chart and $\frac{2}{3}\frac{I_c/L_c}{I_b/L_b}$ adjusted by the factor

$$(3EI_bZ/L_b + 1) \tag{4.7}$$

showed exactly the same result--further substantiating Eq. (4.6).

The factor given in Eq. (4.7) which adjusted G for semi-rigid connections is valid only for the case when the connections are in the inelastic range. If the connections are in the elastic range, then an analysis similar to that performed above indicates that the adjustment factor would be

$$(2EK_bZ/L_b + 1) \text{ and } (6EI_bZ/L_b + 1) \tag{4.7[a]}$$

for braced and unbraced frames, respectively. In addition, all beams framing into the column would be considered effective.

In Sec. 1.1 a procedure for determining the buckling load of columns with semi-rigid connections as recommended by DeFalco and Marino was described [see Eq. (1.3)]. This procedure, which was developed by Driscoll, assumes that the connections are in the

elastic range, and that a beam stiffness reduction factor given in Eq. (1.3) is applied to both braced and unbraced frames. The inverse of this factor can be compared to Eq. (4.7[a]). Upon examination of these factors using typical values of Z, it was found that the solution recommended by DeFalco and Marino is conservative for the braced case, but unconservative for the unbraced case. This method also is more cumbersome to work with than the theoretical solution presented [Eq. (4.7[a])].

4.3 Discussion of Stability Results

Table 4.2 lists values of P_{cr} obtained by using the theoretical solution given above neglecting the "stub" effect. The values were computed using both the elastic Z and unloading Z from the column tests, the elastic Z values from DeFalco, and the elastic Z obtained from Peterson and Cermak's equations. It can be seen from the table that if the flexibility factor from DeFalco is used without regard to connection angle thickness, the buckling load is greatly overestimated (34 percent for Test I, Z-elastic). A comparison of buckling loads using the elastic A from the test and from Peterson, as might be used when framing to a column flange, shows that Peterson's values underestimate the test values for Tests I and III by 15 percent and 7 percent, respectively, but overestimate the buckling load from Test II by 12 percent. These differences follow the same trend as the flexibility factors did, but the magnitudes of the differences are not as great in the buckling loads. If, however, the beams are framed to the column web, the unloading Z values should be used in computing buckling loads. A comparison of the buckling loads using the unloading Z from the tests and the elastic values from Peterson shows that Peterson's values overestimate the actual buckling loads for all three tests by an average of 15 percent.

In design, an engineer may decide to use G equals 10 for the pinned ends, as stated in AISC, or he may even assume a perfect pin with G equal to infinity. The last two columns in Table 4.2

TABLE 4.2 COMPARISON OF THEORETICAL BUCKLING LOADS

Test Number	P_{cr} test Z-elastic	P_{cr} test Z-unload	P_{cr} DeFalco Z-elastic	P_{cr} Peterson Z-elastic	P_{cr} G = 10	P_{cr} G = ∞
I	195^k	141^k	262^k	166^k	96^k	89^k
II	116^k	116^k	262^k	130^k	96^k	89^k
III	172^k	139^k	262^k	160^k	96^k	89^k

give the values of P_{cr} corresponding to these two cases. From the table it is seen that if either of these procedures is used the buckling load is considerably lower than that which is actually available. Using this procedure would be wasteful by a minimum of 17 percent and use of the theoretical procedure is not very complex for the average engineer.

From this discussion it is seen that use of the Z values from Peterson for connections bolted to the flange of a column will yield satisfactory buckling loads. However, when beams frame into the column webs or when the connection angles are welded to the column more data are needed in order to achieve satisfactory results.

4.4 Discussion of Beam-Column Test

From an elastic analysis using the beam stiffness from Eq. (4.1), it was determined that the moments at the ends of the column due to restraint from the beams was about 30 percent of the moment at the column centerline. The ratio of end moment to centerline moment from the test was approximately 0.27, as shown in Fig. 4.3(a). If the connection of the beams and columns is assumed as rigid, the ratio would be 0.96. The calculated deflections, based on these elastic analyses, are shown in Fig. 4.3(b). As expected, the deflections accounting for the semi-rigid connections compare favorably with the test results in the elastic range.

In order to assess the effect of semi-rigid connections on the performance of the beam-column, it is desirable to find what lateral force, H, the structure could carry with no restraint at the ends and with rigid connections.

According to the 1969 AISC Specification,[1] the design of members subjected to bending in one plane and axial forces must satisfy the following requirements:

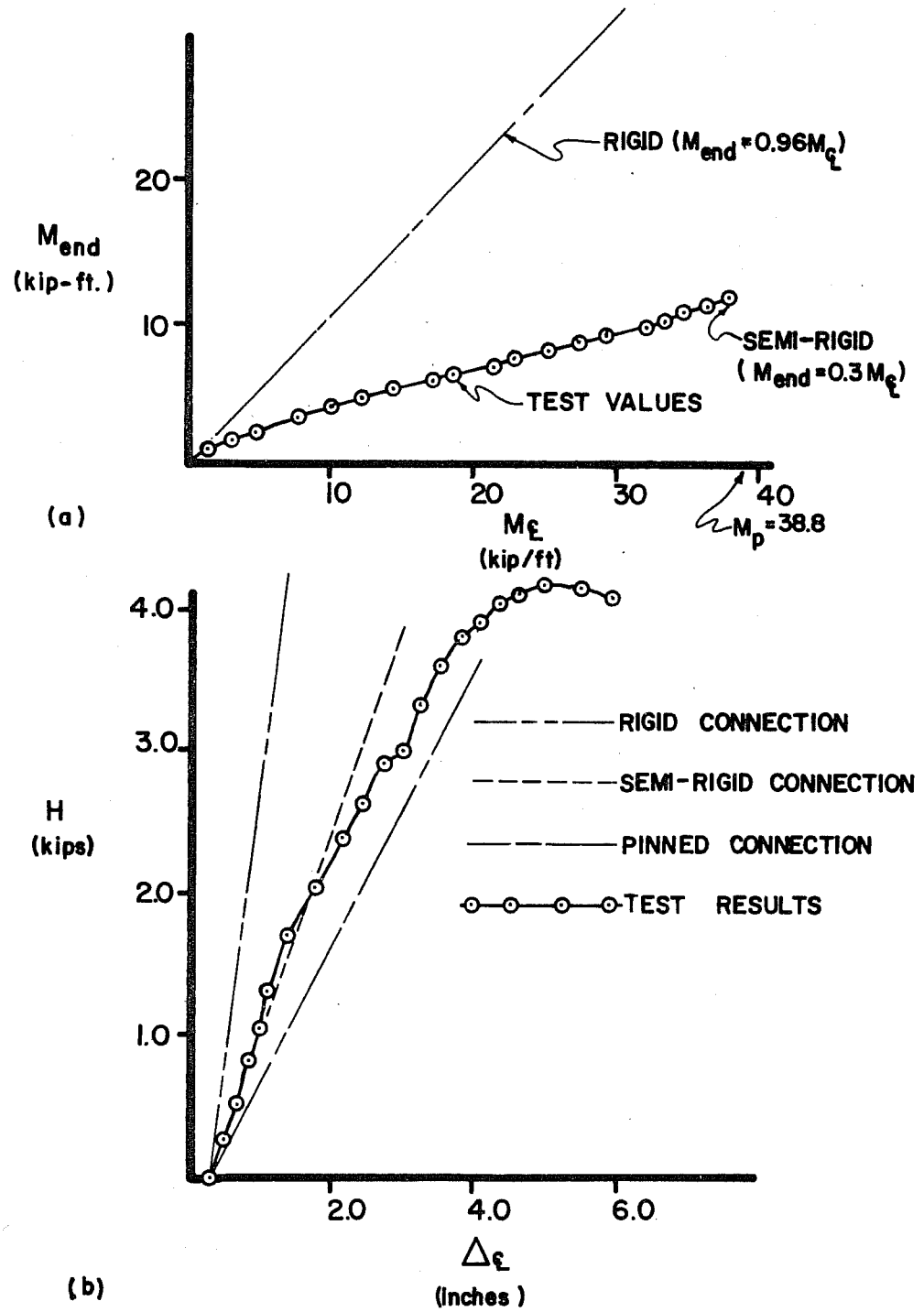

Fig. 4.3 Beam-column behavior

$$\frac{f_a}{F_a} + \frac{C_{my} f_{by}}{(1 - \frac{f_a}{F'_{cy}})F_{by}} \leq 1.0 \qquad (4.8[a])$$

and

$$\frac{f_a}{0.6F_y} + \frac{f_{by}}{F_{by}} \leq 1.0 \qquad (4.8[b])$$

in which $C_m = 1 - 0.2P/P_{cr}$ for the laterally loaded beam-column (see AISC Sprecification for definitions of symbols). The beam-column will be treated as a 20-ft. braced column with restraining beams at each end and laterally braced at midheight. For this beam-column, Eq. (4.8[a]) controls and can be changed to the following ultimate load form (factors of safety removed):

$$\frac{P}{P_{cr}} + \frac{C_m M}{0.83\, M_p (1 - \frac{P}{P_{cr}})} \leq 1.0 \qquad (4.9)$$

where $P_{cr} = \frac{\pi^2 EI_c}{(kL_c)^2}$ and $C_m = 1 - 0.2P/P_{cr}$.

The AISC interaction equation does not permit full plasticity of the cross section when bending occurs about its weak axis. The allowable bending stress is $0.75F_y$, which would be $0.90F_y$ accounting for full plasticity ($0.75/0.90 = 0.83$). Substituting the maximum test values of $P = 50.24$ kips and $M = 172.5$ kip-in. from Test IV, $P_{cr} = 123$ kips from Test I (using the same connection), and the experimental $M_p = 466$ kip-in. from another report[5] into Eq. (4.9) gives $0.415 + 0.699 = 1.114$, which is greater than 1.0. This means that Eq. (4.9) underestimates the actual capacity.

The Structural Stability Research Council[3] permits full plasticity in the bending term resulting in the following interaction equation:

$$\frac{P}{P_{cr}} + \frac{C_m M}{M_p\left(1 - \frac{P}{P_{cr}}\right)} \leq 1.0 \qquad (4.9[a])$$

For the maximum test values, Eq. (4.9[a]) gives 0.415 + 0.581 = 0.996, which is almost exact for this experiment.

From the solution given by Chen,[2] with no residual stress, values of H for a laterally loaded beam-column with pinned ends can also be obtained. The values of H equal to 5.05 kips for no eccentricity of axial load and 4.40 kips for an eccentricity of about 0.7 in. bound the test value of 4.49 kips with an initial eccentricity of 0.3 in. Chen's solution cannot be compared directly with the test results because of the restraining beams.

By setting Eq. (4.9[a]) equal to 1.0 and substituting values of P_{cr} corresponding to no end restraint and restraint of W10X21 beams with rigid connections, and solving for M and H, it is possible to find the lower and upper bounds on H. For no restraint, the allowable H was found to be 1.67 kips, and for rigid connections H equalled 11.4 kips. The test value (4.49 kips) falls in this range and, as would be expected, is closer to the pinned-ends case. From this we see an increase in the amount of lateral load the structure can absorb of 169 percent when Type II connections are considered as semi-rigid rather than pinned.

From the curve in Fig. 4.3(b), it is seen that the maximum lateral load (4.49 kips) occurred at a deflection of 5 in. If the structure is visualized as an unbraced frame with a 10 ft. column and a fixed base, this sway would be unacceptable. In fact, in the author's opinion, the structure would be useless to its inhabitants at a sway deflection of about 2 in. Even this amount of deflection in 10 ft. of height corresponds to a drift index of 0.017, which is 8.5 times the usual service load drift index of 0.002.[9] At 2 in.

of deflection the lateral load was 2.5 kips, which is 56 percent of the maximum load.

In common practice, an elastic analysis would be performed to find the first order moments. With these moments and the interaction equation [Eq. (4.9)] the ultimate lateral load could be obtained. The predicted maximum lateral load is 3.12 kips, which is 25 percent higher than the 2.5 kips corresponding to 2 in. of deflection. We see that this procedure yields an answer that is safe from an ultimate load standpoint, but the structure is rendered useless due to large deflections before this load is reached.

From this discussion we can see that the interaction equations are very good for computing the strength of a structure, but due to the nature of the semi-rigid connections the structure undergoes gross sway deflections before the ultimate strength is reached. Therefore, in designing beam-columns with semi-rigid connections, close attention should be paid to the deflections encountered under design loads. The deflection calculations must account for the semi-rigid behavior of the "simple" connections. Deflections cannot be calculated assuming rigid type connections.

CHAPTER 5

SUMMARY AND RECOMMENDATIONS

The effect of "semi-rigid" beam-to-column connections on column strength has been investigated by tests and a theoretical study. The experimental program consisted of three stability tests and one beam column test conducted on two full-size specimens. The main variables considered were configuration of the web angles used in the connection and their connection to the column web. Three tests were also performed to obtain the moment-rotation characteristics of the various connections.

The rotational resistance factors, Z, obtained from the M-θ tests were then compared to those values from the actual experiments and theoretical predictions. The elastic Z values found from the M-θ tests agreed reasonably with those from the stability experiments. The values from both kinds of tests indicated stiffer joints than the theoretical predictions of Peterson and Cermak. The unloading stiffness from the M-θ tests were much greater than those from the experiments. This difference was attributed to the fact that the beam was attached to a column flange in the M-θ tests rather than the thin column web, as in the major experiments. From the differences in the rotational resistance factors for the different connections, it is apparent that the connection to the column rather than the beam has the most effect on the stiffness of the joint. In general, it was seen that as the distance from the heel of the angle to its point of connection to the column increases the stiffness decreases.

For the stability tests, an "exact" theoretical analysis was performed, accounting for the "semi-rigid" characteristics of the connections as well as the "stub" column portions of the test assemblage. The values of buckling load obtained from the tests agreed favorably with the theoretical values. From the moment-rotation curves from the major experiments, it was apparent that only one beam was restraining the end of the column against rotation, and that it was restraining with a stiffness that was less than the elastic value due to connection to the relatively thin column web. It was found that the theoretical procedure developed was easier and more accurate than that procedure outlined by DeFalco and Marino.

The calculated deflections of the beam-column, based on an elastic analysis with semi-rigid connections ($M_{end} = 0.3M_{\ell}$), showed favorable agreement with the test values. It was shown that the AISC interaction equation, with factors of safety removed, underestimated the strength of the beam-column by 11 percent, but the CRC interaction equation was almost exact. The use of semi-rigid connections enables the beam-column to carry a lateral load about 2.7 times the load allowed assuming no restraint. Gross deflections (5 in. in 10 ft.) were incurred by the beam-column at the ultimate load and at a failure limit of 2 in. the lateral load was only 56 percent of the maximum load.

5.1 Recommendations

Based on the results of the tests and the theoretical analysis presented, a new technique for the design of columns in frames with semi-rigid, Type II connections is recommended. For determination of k, the effective length factor, from the CRC alignment charts use:

$$G = \left(\frac{3EI_b}{L_b} Z + 1\right)\left(\frac{EI_c/L_c}{FEI_b/L_b}\right)$$

where F is a factor that accounts for the actual beam stiffness versus the beam stiffness assumed in the development of the alignment chart (for the braced case F = 1.5; for unbraced frames F = 0.5), and Z equals the value obtained from Peterson and Cermak's procedure for connection to the column flange. In this equation only one beam should be considered to offer restraint at a joint. This recommendation is applicable when the connections are loaded into the inelastic range. An example problem using this procedure is presented in Appendix D.

In designing beam-columns with Type II connections, use of the interaction equations gives good results for computing the strength of the structure. However, close attention should be paid to the deflections encountered under design loads. Deflections should be calculated accounting for the semi-rigid behavior of the connections, not computed assuming rigid type connections.

For connection to a column web or welding of the column connected leg of the connection angle, more data are needed before design recommendations can be introduced.

A P P E N D I X A

NOTATION

A	Cross-sectional area of the section
b_f	Flange width
d	Depth of section
E	Modulus of elasticity for steel (29000 ksi)
F	Factor accounting for difference between actual beam stiffness and stiffness assumed in development of alignment charts equal to: 1.5 braced frame, 0.5 unbraced frame
G	Factor for each end of a column--needed to determine effective length factor, equal to (column stiffness)/(beam stiffness), where each stiffness represents the sum of the stiffnesses in the plane of buckling of the beams or columns which frame into the joint in question
H	Lateral load applied to beam-column
H_{max}	Maximum applied lateral load
I	Moment of inertia of a member
k	Column effective length factor
L	Length of a member; equal to center-to-center distance of beams for the column in a specimen
L_{stub}	Distance above cross-sectional centerline of beams where axial load is applied; equal to 11 in. for all specimens
M	Beam moment level during each loading stage during tests
M_o	Beam moment at start of axial loading. Additional subscripts (M_{oe}, M_{ow}) refer to beams on east or west side of column
M_p	Plastic moment capacity of section
P	Column axial load at each load stage in tests
P_{cr}	Column buckling load
P_E	Euler buckling load; equal to $\pi^2 EI/L^2$
P_{theory}	Theoretical column buckling load based on theoretical analysis accounting for "semi-rigid" connections and "stub" column portion of specimen
t_f	Thickness of flange
t_w	Thickness of web
Z	Flexibility factor for "semi-rigid" connections

$\Delta_{\mathbb{C}}$ Column centerline deflection measured from a line between the geometric center of each joint; equal to $\delta_o + \delta$ at each load stage

δ Deflection at column centerline due to applied beam loads and axial loads

δ_o Initial column centerline eccentricity measured from a line between the geometric center of each joint

θ Rotation of beam at the joint at each load stage; rotation of the end of the beam at the start of column axial loadings

A P P E N D I X B

M-θ TEST SETUP

Figure B-1 shows the setup of the M-θ tests. A W10x21 beam was attached to a reaction frame using each of the connections A, B, and C. It was loaded 116-1/8 in. from the face of the reaction frame by a hydraulic ram. The loads were obtained from a load cell mounted beneath the ram. From these loads the moments at the connections for each load stage were found. Level bubble inclinometers were used to record rotations of the joint and the reaction frame. Subtracting the frame's rotation from the recorded joint rotation gives the true rotation that the connection goes through due to a given amount of moment.

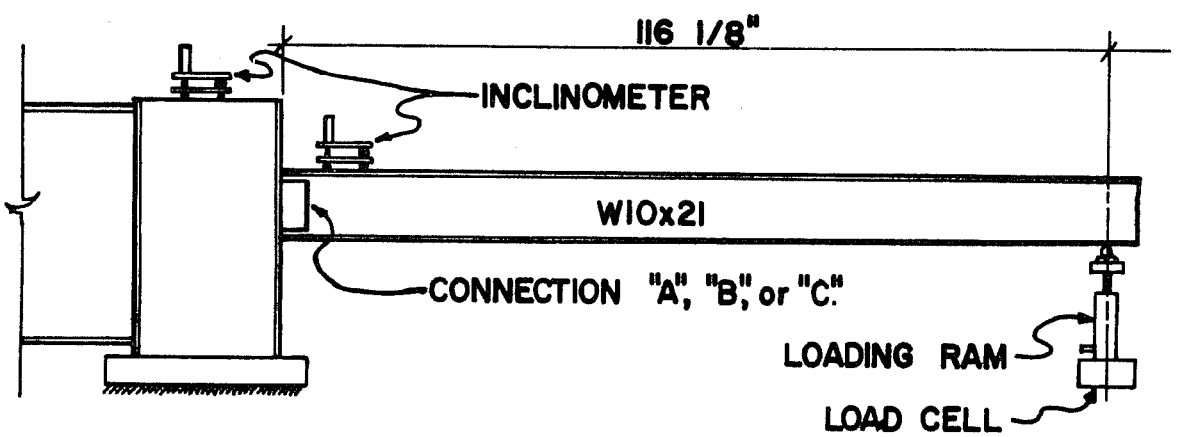

Fig. B-1 M-θ test setup

A P P E N D I X C

EXAMPLE CALCULATION OF Z USING PETERSON AND CERMAK TECHNIQUE

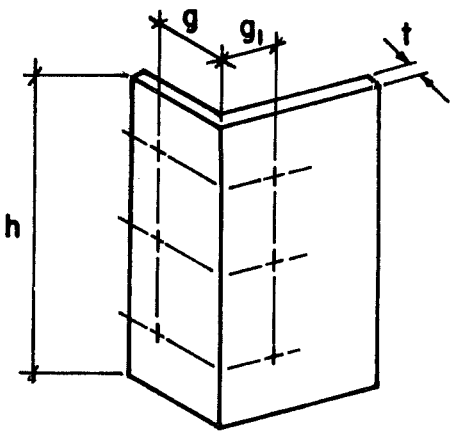

$$Z = \frac{3g_1 + t}{2EhtY^2} n' \qquad \text{(C1)}$$

$$Y = \frac{\sqrt{n'}}{1 + \sqrt{n'}} h \qquad \text{(C2)}$$

$$n' = \frac{4g^3}{t^2(g_1 + t)} \left(\frac{g + g_1}{4g + g_1} \right) \qquad \text{(C3)}$$

E = Modulus of elasticity equals 29000 ksi

g = Gage distance from heel of angle to connector centerline on column-connected leg of angle

g_1 = Gage distance from heel of angle to connector centerline on beam-connected leg of angle

h = Total height of angle

t = Nominal thickness of angle

For Connection A

g = 2.375 in.

g_1 = 2.5 in.

h = 8 in.

t = 0.25 in.

$$n' = \frac{4g^3}{t^2(g_1+t)} \left(\frac{g + g_1}{4g + g_1}\right) = \frac{4(2.375)^3}{(0.25)^2(2.5 + 0.25)} \left(\frac{2.375 + 2.5}{4 \times 2.375 + 2.5}\right) = 126.7$$

$$Y = \frac{\sqrt{n'}}{1 + \sqrt{n'}}\, n = \frac{\sqrt{126.7}}{1 + \sqrt{126.7}} \times 8 = 7.35$$

$$Z = \frac{3(g_1 + t)}{2EhtY^2}\, n' = \frac{3}{2} \times \frac{2.5 + 0.25}{(29000)(8)(0.25)(7.35)^2} \times 126.7$$

$$= \underline{\underline{1.67 \times 10^{-4} \text{ rad/kip-in.}}}$$

A P P E N D I X D

EXAMPLE PROBLEM USING PROPOSED DESIGN PROCEDURE

Example #1 from DeFalco[4]

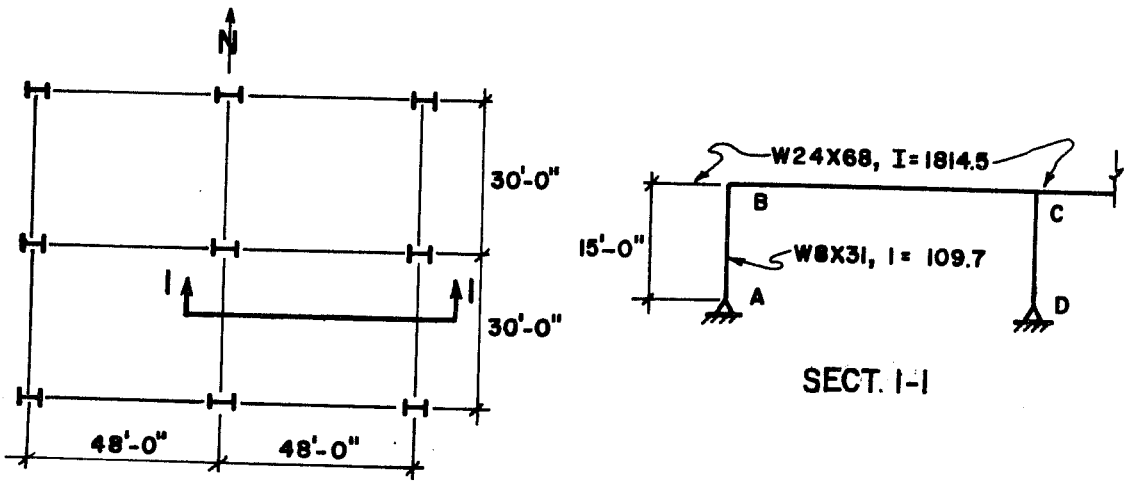

Determine the effective length factor for column A-B

Given: (1) No lateral bracing in E-W direction
(2) Many bays in E-W direction; i.e., framed connections provide sufficient moment capacity to resist moments from lateral forces
(3) All columns receive restraint against sidesway in N-S direction
(4) Same connections used as are used in DeFalco; i.e., $Z = 0.20 \times 10^{-5}$ rad/k-in.

Solution:

$$Z = 0.20 \times 10^{-5} \text{ rad/k-in.}$$

$$G_{top} = \left[\frac{3EI_b}{L_b} Z + 1\right]\left[\frac{EI_c/L_c}{F\ EI_c/L_c}\right] \qquad E = 29000 \text{ ksi} \qquad F = 0.5$$

$$= \left[\frac{3(29000)(1814.5)(0.2\times10^{-5})}{(48' \times 12")} + 1\right]\left[\frac{109.7/15}{0.5(1814.5/48)}\right]$$

$$= [1.55][0.387] = 0.60$$

$$G_{bot} = 10$$

$$\underline{\underline{k = 1.82}}$$

$$P_{cr} = \frac{\pi^2 EI_c}{(kL_c)^2} = \frac{\pi^2(29000)(109.7)}{(1.82 \times 180)^2} = 293^k$$

Using DeFalco procedure, $P_{cr} = 330^k$

REFERENCES

1. American Institute of Steel Construction, Specification for the Design, Fabrication, and Erection of Structural Steel for Buildings, New York, 1969.

2. Chen, W. F., "Further Studies of Inelastic Beam-Column Behavior," Journal of the Structural Division, Proc. ASCE, 97, ST2, February 1971, pp. 529-544.

3. Column Research Council, Guide to the Design of Compression Members, Second Edition, John Wiley and Sons, Inc., New York, 1960.

4. DeFalco, F., and Marino, F. J., "Column Stability in Type 2 Construction," Engineering Journal, American Institute of Steel Construction, April 1966, pp. 67-71.

5. Laosirichon, V., "The Effect of Beam Yielding on Steel Column Strength," Ph.D. dissertation, The University of Texas at Austin, August 1975.

6. Lothers, J. E., "Elastic Restraint Equations for Semi-Rigid Connections," Transactions ASCE, Vol. 116, No. 2437, 1951, pp. 480-494.

7. Peterson, D. F., Jr., and Cermak, J. F., Discussion of Ref. 6, Vol. 116, 1951, pp. 496-499.

8. Ramirez, D. R., "The Effect of Beam Yielding on the Stability of Columns," M.S. thesis, The University of Texas at Austin, January 1975.

9. Tall, Lambert (Editor in Chief), Structural Steel Design, Second Edition, The Ronald Press Company, New York, 1964, pp. 720-721, 730.

10. Timoshenko, S. P., and Gere, J. M., Theory of Elastic Stability, McGraw-Hill Book Company, New York, 1961.

11. Class Notes (C.E. 397K), "Stability of Structures," The University of Texas at Austin, 1975.